Fundamental Initial Frequency and Frequency Rate Estimation of Random-Amplitude Harmonic Chirps

Yaron Doweck, *Student Member, IEEE*, Alon Amar, *Member, IEEE*, and Israel Cohen, *Fellow, IEEE*

***Abstract*—We consider the problem of estimating the fundamental initial frequency and frequency rate of a linear chirp with random amplitudes harmonic components. We develop an iterative nonlinear least squares estimator, which involves a large number of computations as it requires high resolution search in the initial frequency and frequency rate parameter space. As an alternative, we suggest two suboptimal low-complexity estimators. The first is based on the high-order ambiguity function, which reduces the problem to a one-dimensional search. The second method applies our recently published harmonic separate-estimate method, which was used for constant-amplitude harmonic chirps. We present modifications of both methods for harmonic chirps with random amplitudes. We also provide a framework for estimating the number of harmonic components. Numerical simulations show that the iterative nonlinear least-squares estimator achieves its asymptotic accuracy in medium to high signal-to-noise ratio, while the two sub-optimal low-complexity estimators perform well in high signal-to-noise ratio. Real data examples demonstrate the performance of the harmonic separate-estimate method on random amplitude real-life signals.**

***Index Terms*—Harmonic chirps, multiplicative noise, random amplitude chirps.**

I. Introduction

CHIRP parameter estimation has many applications in signal processing, as chirps are very common in sonar, radar, communication, speech and echolocations calls. A common assumption in chirp analysis methods is that the amplitude of the signal is constant during each observation time. The problem of analyzing constant-amplitude chirp signals has received much attention in literature. The higher-order ambiguity function (HAF) is commonly used for parameter estimation of such signals, e.g., [1]–[3]. Other techniques include the high-order phase function [4], [5], nonlinear least-squares estimator (NLSE) [6], multi-linear method [7], quasi-maximum-likelihood [8] or by using time-frequency representations such as the Wigner-Ville distribution [9] or the fractional Fourier transform [10].

In some applications such as radar, sonar and communication, distortions caused by scattering, fluctuations or multi-path phenomena result in a signal with time-varying amplitude [11]–[15]. Chirps with random amplitude are also used to model formants in speech processing applications [16], [17], electric currents in induction motor fault analysis [18], and animals sounds (bats, whales, dolphins, birds etc.).

Previous work on the analysis of time-varying amplitude signals can be divided into two cases. The first case focuses on complex exponential signals (i.e., constant frequency). Frequency estimation for such signals can be achieved using cyclic moments [11], least-squares (LS) [12] and NLSE [19], [20], subspace methods [21], high-order spectra [22], [23] and pulse-pair method [24]. The second case, which received significantly less attention, considers the model of a mono-component chirp with time-varying amplitude. Methods for parameter estimation of such signals include the cyclic moment approach [13], [16], NLSE and HAF-based estimation [15], high-order instantaneous moments [25] and the Wigner-Ville distribution-based methods [26], [27].

Herein, we consider a class of multi-component chirps, where the components satisfy a harmonic relation. For example, Fig. 1 presents three types of calls, produced by *E. Nilssonii* bat [28], *G. melas* whale [29] and *Hippolais icterina* bird [30], showing harmonic chirp signals with random amplitude. The frequency of each component is an integer multiple of the time-varying frequency of a fundamental chirp. Such harmonic signals occur due to propagation through a nonlinear media such as rotating machinery in vibrational analysis, music and formants in audio and speech processing, electrical power systems, and target localization [31], [32]. In some cases, for example, in active transmission used in tissue harmonic imaging in ultrasound [33] or by mammals [34], [35] (e.g., bats, dolphins, whales) the signal is deliberately transmitted as a sum of harmonic chirps to increase the detectability of the source of interest.

We further assume that in each observation window, the components can be approximated as a linear frequency modulated (LFM) chirp signal. Previous solutions for the analysis of harmonic series assume that the frequency is constant in each observation window, thus setting a limit on the possible segment length. Assuming such a model of time-varying frequency enables us to increase the segment length and consequently improve the estimation accuracy. As opposed to multi-component signal, the harmonic components problem only involves estimating the parameters of the fundamental chirp, as we only estimate the initial frequency and frequency rate of the fundamental chirp.

We first present an iterative process by extending the NLSE presented in [15] for mono-component chirp with random amplitude, to the current case of a harmonic LFM signal with a known number of components, which we term the iterative har-

Manuscript received March 22, 2015; revised June 17, 2015 and July 19, 2015; accepted July 24, 2015. Date of publication July 31, 2015; date of current version October 26, 2015. The associate editor coordinating the review of this manuscript and approving it for publication was Prof. Hongbin Li. This research was supported by the Israel Science Foundation (grant no. 1130/11).

Y. Doweck and I. Cohen are with the Department of Electrical Engineering, Technion—Israel Institute of Technology, Technion City, Haifa 32000, Israel (e-mail: yarond@tx.technion.ac.il; icohen@ee.technion.ac.il).

A. Amar is with the Signal Processing Department, Acoustics Research Center, Rafael, Haifa 3102102, Israel (e-mail: alonamar@rafael.co.il).

Color versions of one or more of the figures in this paper are available online at http://ieeexplore.ieee.org.

Digital Object Identifier 10.1109/TSP.2015.2463251

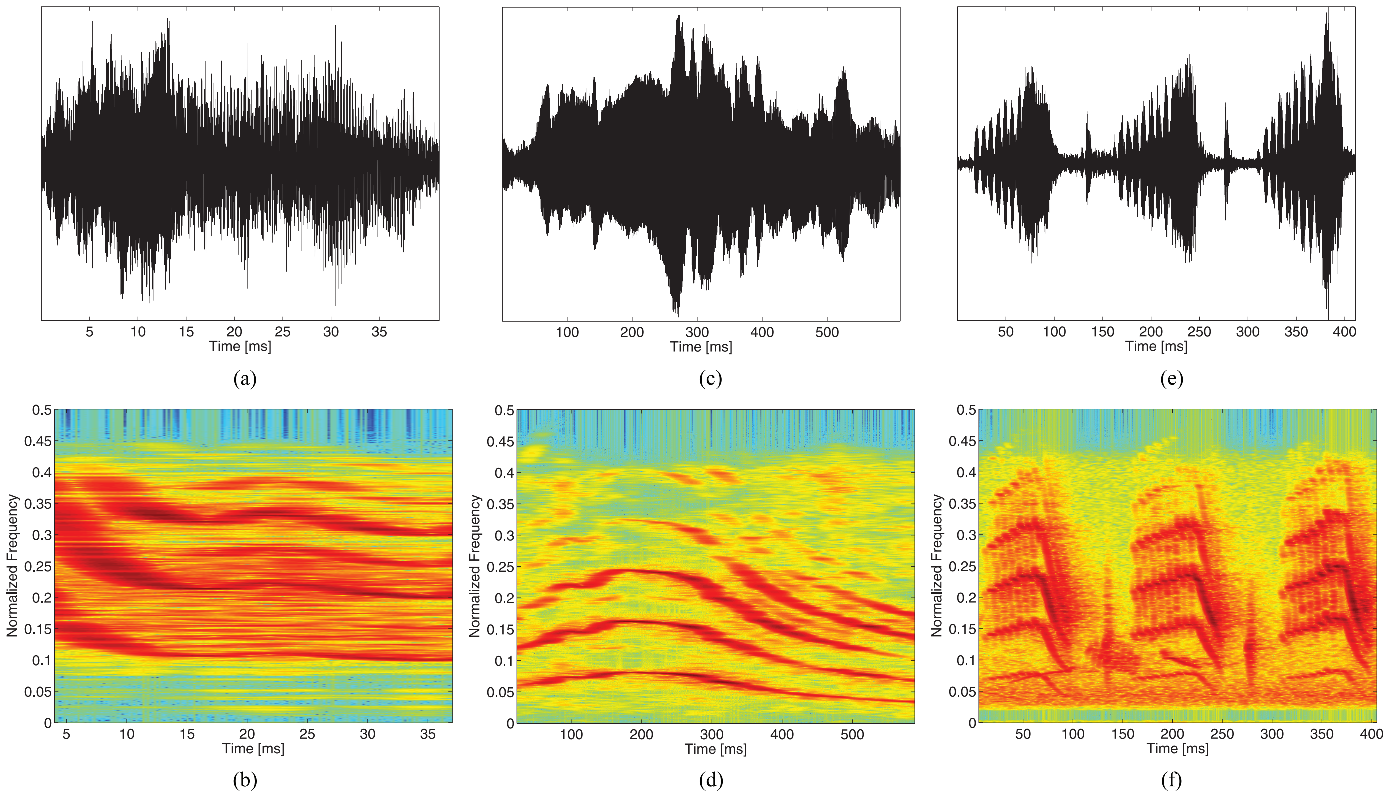

Fig. 1. Examples of animal harmonic chirps. Time domain samples and spectrogram of (a),(b) an echolocation call produced by an *E. Nilssonii* bat, (c),(d) an echolocation call produced by a *G. melas* whale, and (e),(f) a call of a *Hippolais icterina* bird.

monic-NLSE (IHNLSE). We then suggest a framework to determine the number of harmonic components using peakedness measures evaluated for the spectrum of the signal. IHNLSE requires exhaustive search in the initial frequency-frequency rate space. We show that, in order to achieve the optimal accuracy, a search resolution of $N^{3/2}$ and $N^{5/2}$ is required for the initial frequency and frequency rate, respectively, where N is the number of samples. We further propose two low-complexity estimators to avoid such a search. The first is a modification of the HAF-based estimation method [15]. The second is a modification of the harmonic separate-estimate (Harmonic-SEES) method [36], [37] for random-amplitude harmonic chirps, which we term the harmonic random separate-estimate (HRA-SEES). The Harmonic-SEES method is a low-complexity estimator based on the separate-estimate approach, used for estimating the coefficients of constant modulus signals [38], [39].

The Harmonic-SEES method was presented in [36] for parameter estimation of constant-amplitude harmonic linear chirps. The Harmonic-SEES method consists of two steps. First, the signal is separated to its harmonic components using a coarse parameter estimation. Next, the parameters are estimated from the phases of all the components using a recursive phase unwrapping and least-squares estimation. Similarly to NLSE and HAF-based estimator, in order to use the Harmonic-SEES method on random-amplitude chirp, we use the squared signal. We then modify the Harmonic-SEES steps to suit the transformed signal. The Harmonic-SEES, and consequently HRA-SEES, are similar in a way to the analysis of chirps using the Radon-Wigner transform [40], which applies the Radon transform to the Wigner-Ville distribution of the signal, and the Radon-ambiguity transform [41] which applies the Radon transform to the ambiguity function of the signal.

We show that both methods can be successfully modified for harmonic LFM signals with unknown number of harmonic components. Simulations show that IHNLSE achieves its analytic asymptotic accuracy in medium to high signal-to-noise ratio (SNR) and that both low-complexity methods yield good estimation results for high SNR. Two real-data examples demonstrate the application of HRA-SEES method to echolocation calls.

II. The Signal Model

Consider a discrete-time signal composed of M attenuated harmonic components observed in the presence of noise,

$$x[n] = \sum_{m=1}^{M} a_m[n] s_m[n;\boldsymbol{\theta}] + v[n],\ n = 0,\ldots,N-1 \tag{1}$$

where $a_m[n]$ is the random amplitude of the mth harmonic. The signal $v[n]$ is a white Gaussian discrete-time process representing the zero mean additive noise with a known variance σ_v^2, uncorrelated with the amplitudes. We assume that the amplitudes can be described as $a_m[n] = \alpha_m[n]e^{j\varphi_m}$, where $\alpha_m[n]$ is a real time-varying process and φ_m is the constant phase of the m'th component. We do not assume any other kind of model for the amplitudes. This is a generalization of the signal model presented in [15], for multi-component signal. The number of harmonics, M, is not assumed to be known a-priori. The discrete-time mth harmonic component signal is

$$s_m[n;\boldsymbol{\theta}] = e^{j2\pi m(\theta_1 n + \frac{1}{2}\theta_2 n^2)},\ \begin{matrix} n = 0,\ldots,N-1 \\ m = 1,\ldots,M \end{matrix} \tag{2}$$

where $\boldsymbol{\theta} = [\theta_1, \theta_2]^T$ is the parameters vector of the normalized initial frequency and normalized frequency rate. For simplicity, all frequencies mentioned hereafter are assumed to be normalized by the sampling rate, F_s, unless otherwise stated. Thus, the sampling rate is set to $F_s = 1$.

A special case of the assumed model is the constant-amplitude harmonic chirps, where $\alpha_m[n] \equiv \alpha_m$. This problem was addressed in [36] and two sub-optimal low-complexity estimation methods were suggested, the Harmonic-SEES and a modified HAF-based estimation. The problem we address herein is: Given the samples of an harmonic LFM signal with random amplitudes, $x[n]$, estimate the unknown parameter vector, $\boldsymbol{\theta}$, and the model order, M.

III. Mono-Component NLSE

We present NLSE of the parameters of harmonic linear chirp with random amplitudes. We start by presenting the estimator for a mono-component LFM with a random amplitude [15]. Next, we show that the maximization involved in the mono-component case cannot be solved for a multi-component signal and provide a motivation for the iterative approach presented in the next section.

To start, consider a single LFM with a constant amplitude

$$x[n] = as[n;\boldsymbol{\theta}] + v[n] \tag{3}$$

where $s[n;\boldsymbol{\theta}] = e^{j2\pi(\theta_1 n + \frac{1}{2}\theta_2 n^2)}$ and a is a complex constant amplitude. The maximum likelihood estimator (MLE) of $\boldsymbol{\theta}$ is given by [36]

$$\begin{aligned}\hat{\boldsymbol{\theta}} &= \arg\max_{\boldsymbol{\theta}} \frac{1}{N}\left|\sum_{n=0}^{N-1} x[n]e^{-j2\pi(\theta_1 n + \frac{1}{2}\theta_2 n^2)}\right|^2 \\ &\triangleq \arg\max_{\boldsymbol{\theta}}\, Q(x,\boldsymbol{\theta}).\end{aligned} \tag{4}$$

We see that the MLE is based on considering the maximum of the squared absolute of a matched filtering process where the signal $x[n]$ is matched to a complex conjugate chirp with the same model as the original chirp signal. An intuitive explanation of this estimator can be given be examining the values of $Q(x, \boldsymbol{\theta})$ at its maximum, the point where $\hat{\boldsymbol{\theta}}$ equals the true parameters of the signal, $\boldsymbol{\theta}$. In the absence of noise we get, by substituting (1) with $M = 1$ into (4), that

$$Q(x,\boldsymbol{\theta}) = \frac{1}{N}\left|\sum_{n=0}^{N-1} a\right|^2 = Na^2 \tag{5}$$

which is the entire energy of the signal.

We now generalize the previous case and consider a single chirp with random amplitude. The chirp parameters, $\boldsymbol{\theta}$, and amplitude, $a[n]$, can be estimated using nonlinear least-squares (NLS) approach by minimizing the following criterion [15]

$$\hat{\boldsymbol{\theta}}, \hat{a}[n] = \arg\min_{\boldsymbol{\theta}, a[n]} \left|\sum_{n=0}^{N-1} x[n] - a[n]e^{-j2\pi(\theta_1 n + \frac{1}{2}\theta_2 n^2)}\right|^2. \tag{6}$$

By taking the derivatives with respect to (w.r.t.) $a[n]$ and $\boldsymbol{\theta}$,and equating to zero, NLSE for the chirp parameters is [15, Appendix A]

$$\begin{aligned}\hat{\boldsymbol{\theta}} &= \arg\max_{\boldsymbol{\theta}} \frac{1}{N}\left|\sum_{n=0}^{N-1} x^2[n]e^{-j2\pi\cdot 2(\theta_1 n + \frac{1}{2}\theta_2 n^2)}\right| \\ &\triangleq \arg\max_{\boldsymbol{\theta}} \frac{1}{N} L(x,\boldsymbol{\theta}).\end{aligned} \tag{7}$$

From (7) it is clear that NLSE for $\boldsymbol{\theta}$ has a similar structure as MLE in (4) with two modifications: (1) the values of the chirp parameters are twice that of the original chirp, (2) the chirp is matched to $x^2[n]$ instead of $x[n]$ as with MLE. The value of NLSE at its maximum ignoring noise is given by

$$L(x,\boldsymbol{\theta}) = \left|\sum_{n=0}^{N-1} a^2[n]\right| = E_s \tag{8}$$

where E_s is the energy of the signal. When the amplitude is a random process, the squaring of the signal in NLSE results in the energy of the signal just as in MLE. That is, NLSE extends the idea of MLE to signals with random amplitude.

IV. Harmonic Components NLSE

We now consider the case of harmonic chirp. We start by assuming that the number of harmonic components, M, is known. Similar to the estimator in (6), we define NLS criterion, using (1), as

$$\begin{aligned}&\hat{\boldsymbol{\theta}}, \{\hat{a}_m[n]\}_{m=1}^M \\ &\quad = \arg\min_{\boldsymbol{\theta}, \{a_m[n]\}_{m=1}^M} \left|\sum_{n=0}^{N-1}\left(x[n] - \sum_{m=1}^M a_m[n]s_m[n;\boldsymbol{\theta}]\right)\right|^2.\end{aligned} \tag{9}$$

Attempting to take the derivatives w.r.t. $a_m[n]$ for each n and m and equate the results to zero yields a set of N equations with $M \cdot N$ unknowns, which is an under-determined problem. For a single component LFM, on the other hand, taking the derivatives of (6) w.r.t. $a[n]$ yields a set of N equations with N unknowns, which guaranties a solution to (6). Note that if we were to assume a specific model of the amplitudes, with a parameters vector λ, then (9) can be optimized w.r.t. λ [15].

We therefore wish to adapt the main idea of NLSE solution for mono-component chirp, which is based on squaring the signal before the estimation process, in order to sum its entire energy. For that purpose, we first explore the form of $x^2[n]$ in the multi-component case,

$$\begin{aligned}x^2[n] &= \sum_{k,p=1}^M a_k[n]a_p[n]s_k[n;\boldsymbol{\theta}]s_p[n;\boldsymbol{\theta}] \\ &\quad + 2\sum_{m=1}^M a_m[n]s_m[n;\boldsymbol{\theta}]v[n] + v^2[n] \\ &= \sum_{m=2}^{2M} \tilde{a}_m[n]s_m[n;\boldsymbol{\theta}] \\ &\quad + 2\sum_{m=1}^M a_m[n]s_m[n;\boldsymbol{\theta}]v[n] + v^2[n]\end{aligned} \tag{10}$$

where

$$\tilde{a}_m[n] = \sum_{k,p=1}^M a_k[n]a_p[n]\mathbb{1}_{k+p=m},\ m = 2,3,\ldots,2M \tag{11}$$

and $\mathbb{1}$ is the indicator function, that equals 1 if $k + p = m$ and 0 otherwise. Since the noise is a zero mean random process and it is uncorrelated with the amplitudes, the product between the harmonic components and the noise is regarded as additional

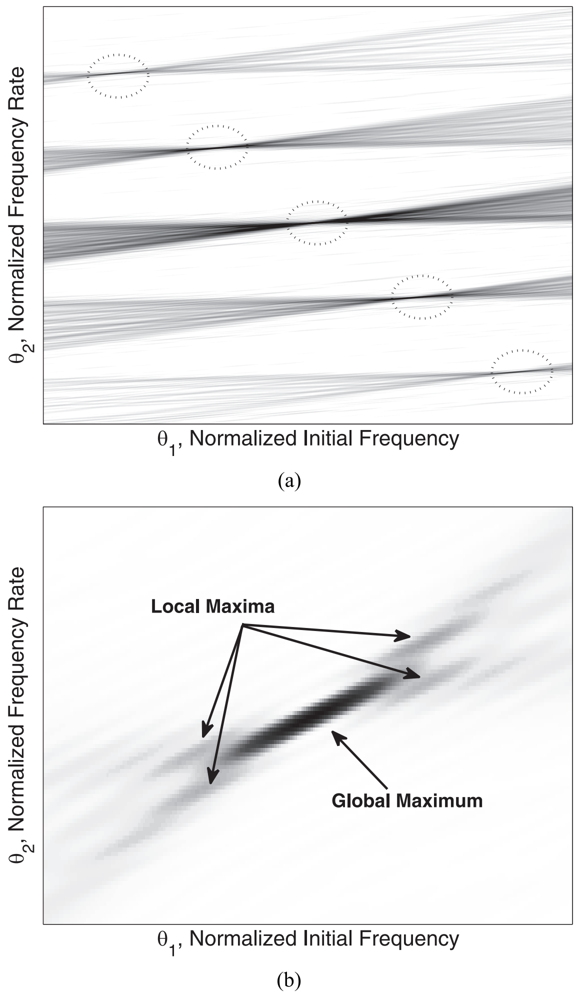

Fig. 2. The NLSE cost function, $L(x, \boldsymbol{\theta})$. (a) The entire range of possible parameters, (b) enlarged area around the strongest peak.

noise rather than a harmonic signal that can be used in the estimation process. We can therefore define

$$x^2[n] = \sum_{m=2}^{2M} \tilde{a}_m[n] s_m[n; \boldsymbol{\theta}] + \tilde{v}[n] \tag{12}$$

where $\tilde{v}[n]$ is composed of the squared noise, $v^2[n]$, and all the products in (10) between the noise and the harmonic components. Note that in low SNR, by squaring the signal the noise is actually amplified and we can expect degraded performance. It can be seen that $x^2[n]$ is composed of $2M-1$ LFM components where the first component has parameters that are twice that of the original fundamental LFM. That is, $2M-1$ harmonic LFM components with the fundamental chirp absent. Clearly, squaring the signal imposes a constraint on the possible range for the parameters. In order to avoid aliasing, we assume that the initial frequency and frequency rate satisfy that $f_{\max} < 1$, where $f_{\max} = 2M\theta_1$ or $f_{\max} = 2M(\theta_2 + N\theta_2)$ for decreasing or increasing chirp, respectively.

Example 1: As an illustrative example, consider the case of a fundamental LFM where $\theta_1 = 0.1$, $\theta_2 = 10^{-5}$, $N = 1024$. The number of harmonic components is $M = 3$ and the amplitudes are generated as an independent Gaussian processes with mean 1 and variance 0.25 each. The NLSE cost function defined in (7), $L(x, \boldsymbol{\theta})$, is presented in Fig. 2(a). There are five peaks, marked in circles, corresponding to the five harmonic components in $x^2[n]$. The peaks are well separated. In a close region around each peak, $L(x, \boldsymbol{\theta})$ is similar to that of a single component signal. Surrounding each peak there are a few minor peaks. Fig. 2(b) shows a small area around the strongest peak, surrounding the local maxima. These peaks can be higher than those belong to the other components, as is the case with the strong peak in the middle. Due to the presence of these minor peaks, it is impossible to estimate the parameters by simply locating the $2M-1$ highest peaks in $L(x, \boldsymbol{\theta})$. A possible estimation approach is suggested in the next section.

V. Iterative NLSE for Harmonic Chirps

We suggest an iterative approach based on NLSE for a single component chirp, which we term for simplicity as IHNLSE. We start by presenting an estimator and derive its asymptotic bias and variance under the assumption that the number of components is known . Next, we show how peakedness measures of the spectrum of the signal can be used to estimate the number of components when it is unknown.

A. Known Model Order

Recall that $L(x, \boldsymbol{\theta})$ has $2M-1$ peaks corresponding to the harmonic components in $x^2[n]$. At each iteration, the global maximum of $L(x, \boldsymbol{\theta})$ is located. Then, the component corresponding to the peak found is filtered from the signal using a de-modulation and filtering scheme proposed in [42]. Note that standard band-pass linear filtering cannot be applied since the harmonic components may overlap in frequency.

More specifically, we use $x_1[n] = x^2[n]$ and estimate its strongest component using (7). The estimated parameters are denoted by $\hat{\boldsymbol{\theta}}^{(1)} = [\theta_1^{(1)}, \theta_2^{(1)}]$. Next, we wish to filter the components whose parameters were found from the signal, so that in the next iteration, $L(x, \boldsymbol{\theta})$ will not have a global maximum at $\hat{\boldsymbol{\theta}}^{(1)}$. The random amplitude is not estimated, therefore we cannot reconstruct the component and subtract it from the signal. The estimated parameters, $\hat{\boldsymbol{\theta}}^{(1)}$, are used to construct the normalized chirp

$$s[n; 2\hat{\boldsymbol{\theta}}^{(1)}] = e^{j2\pi \cdot 2(\theta_1^{(1)} n + \frac{1}{2}\theta_2^{(1)} n^2)}. \tag{13}$$

In order to filter the estimated component, the signal is modulated by $s^*[n; 2\hat{\boldsymbol{\theta}}^{(1)}]$, filtered with a high-pass filter designed to remove frequencies around zero and then modulated back by $s[n; 2\hat{\boldsymbol{\theta}}^{(1)}]$. The resulted signal is given by

$$x_2[n] = ((x_1[n] s^*[n; 2\hat{\boldsymbol{\theta}}^{(1)}]) * h[n]) s[n; 2\hat{\boldsymbol{\theta}}^{(1)}] \tag{14}$$

where $h[n]$ is the high-pass filter and $*$ denotes convolution. Note that the random amplitudes are not subtracted from the signal, only their chirp modulation. The resulted signal can be approximated as

$$x_2[n] \approx \sum_{m \neq p} \tilde{a}_m[n] s_m[n; \boldsymbol{\theta}] + \bar{a}_p[n] + \tilde{v}[n] \tag{15}$$

where

$$\bar{a}_p[n] = ((\tilde{a}_p[n] s^*[n; 2\hat{\boldsymbol{\theta}}^{(1)}]) * h[n]) s[n; 2\hat{\boldsymbol{\theta}}^{(1)}] \tag{16}$$

for some $p \in \{2, \ldots, 2M\}$. We assume that filtering any signal, $y[n]$, with $h[n]$ yields $y[n] * h[n] \approx y[n] - 1/N \sum_{n=0}^{N-1} y[n]$. Therefore

$$\bar{a}_p[n] \approx \tilde{a}_p[n] - \mu_{\tilde{a}_p} \tag{17}$$

where $\mu_{\tilde{a}_p} = E\{\tilde{a}_p[n]\}$. The process is repeated with $x_2[n]$ to obtain $\hat{\boldsymbol{\theta}}^{(2)}$ and so on, with a total of $2M - 1$ times to obtain the set $\hat{\boldsymbol{\theta}}^{(1)}, \ldots, \hat{\boldsymbol{\theta}}^{(2M-1)}$. Since the number of components, M, is assumed to be known, the stopping condition for the iterative process is also known (i.e., after $2M - 1$ iterations). If this assumption does not hold then a stopping condition, or model order selection rule, is required. This matter is discussed in detail later.

Each of the $2M - 1$ vectors estimated above is a multiple of the parameter vector of the fundamental chirp, $\boldsymbol{\theta}$. Thus, the parameters of interest can be estimated by properly averaging the estimated components. But first we have to associate each vector, $\hat{\boldsymbol{\theta}}^{(m)}$, with the right component, as there is no guaranty that it belongs to the m'th component. In order to do so we sort the set of estimated parameters. Similarly to [36], we define a mapping, $f(m) : [2, 2M] \rightarrow [1, 2M - 1]$, such that $\hat{\theta}_1^{(f(2))} < \hat{\theta}_1^{(f(3))} < \cdots < \hat{\theta}_1^{(f(2M))}$. Then, the parameters can be estimated by solving the following LS problem

$$\hat{\boldsymbol{\theta}} = \arg\min_{\boldsymbol{\theta}} \|\mathbf{A}_M \boldsymbol{\theta} - \boldsymbol{\theta}_M\|^2 \tag{18}$$

where

$$\mathbf{A}_M = \begin{bmatrix} \mathbf{g}_M & \mathbf{0}_M \\ \mathbf{0}_M & \mathbf{g}_M \end{bmatrix} \tag{19}$$

where $\mathbf{0}_n$ is the $n \times 1$ vector with all elements equal to zero, $\mathbf{g}_M = [2, \ldots, 2M]^T$ and $\boldsymbol{\theta}_M = [\boldsymbol{\theta}_M^{(1)}, \boldsymbol{\theta}_M^{(2)}]^T$. Where $\boldsymbol{\theta}_M^{(k)} = [\hat{\theta}_k^{(f(2))}, \ldots, \hat{\theta}_k^{(f(2M))}]$, for $k = 1, 2$. Solving the above optimization problem yields

$$\hat{\boldsymbol{\theta}} = (\mathbf{A}_M^T \mathbf{A}_M)^{-1} \mathbf{A}_M^T \boldsymbol{\theta}_M = \frac{1}{C_M} \sum_{m=2}^{2M} m \hat{\boldsymbol{\theta}}^{(f(m))} \tag{20}$$

where $C_M = \sum_{m=2}^{2M} m^2 = \frac{1}{6}(M+1)M(2M+1)$. The complete process is summarized in Algorithm 1.

Algorithm 1: Iterative Harmonic-NLSE (IHNLSE)

Input:
  $x[n]$ – Input signal
  M – Model order
Output:
  $\hat{\boldsymbol{\theta}}$ – Estimated parameters

  $x_1[n] \leftarrow x^2[n]$
  for $m \leftarrow 1, \ldots, 2M - 1$ **do**
    $\hat{\boldsymbol{\theta}}^{(m)} \leftarrow \arg\max_{\boldsymbol{\theta}} L(x_m, \boldsymbol{\theta})$
    $x_{m+1}[n] \leftarrow ((x_m[n] s^*[n; 2\hat{\boldsymbol{\theta}}^{(m)}]) * h[n]) s[n; 2\hat{\boldsymbol{\theta}}^{(m)}]$
  end for
  $\hat{\boldsymbol{\theta}} \leftarrow (\mathbf{A}_M^T \mathbf{A}_M)^{-1} \mathbf{A}_M^T \boldsymbol{\theta}_M = \frac{1}{C_M} \sum_{m=2}^{2M} m \hat{\boldsymbol{\theta}}^{(f(m))}$

B. Accuracy Analysis

We evaluate the accuracy of the proposed IHNLSE by examining its bias and variance. At each step the signal of interest can be expressed as

$$x_p^2[n] = \tilde{a}_p[n] s_p[n; \boldsymbol{\theta}] + \tilde{v}_p[n]. \tag{21}$$

The noise, $\tilde{v}_p[n]$, is composed of the other harmonics as well as the squared noise. Without loss of generality, we assume that the components are estimated in order, i.e., $f(p) = p$. From (10) and (15) it can be seen that, when estimating $\hat{\boldsymbol{\theta}}^{(p)}$, $p = 2, \ldots, 2M$, the noise is given by

$$\begin{aligned}\tilde{v}_p[n] = \sum_{m=2}^{p-1} \bar{a}_m[n] + \sum_{m=p+1}^{2M} \tilde{a}_m[n] s_m[n; \boldsymbol{\theta}] \\ + 2\sum_{m=1}^{M} a_m[n] s_m[n; \boldsymbol{\theta}] v[n] + v^2[n].\end{aligned} \tag{22}$$

We start by deriving the asymptotic bias and variance of $\hat{\boldsymbol{\theta}}^{(p)}$. Assuming the amplitudes, $a_m[n]$, and noise, $v[n]$, are uncorrelated, it can be shown that

$$E\{x_p^2[n]\} = \sum_{m=p}^{2M} \mu_{\tilde{a}_m} s_m[n; \boldsymbol{\theta}]. \tag{23}$$

In order to show that the estimator is asymptotically unbiased, we show that, asymptotically, $L(x_p, \hat{\boldsymbol{\theta}}^{(p)})/N$ achieves a global maximum at $\hat{\boldsymbol{\theta}}^{(p)} = p\boldsymbol{\theta}$ [15]

$$\begin{aligned}L_\infty(x_p, \hat{\boldsymbol{\theta}}^{(p)}) &= \lim_{N\to\infty} \frac{1}{N} \left| L(x_p, \hat{\boldsymbol{\theta}}^{(p)}) \right| \\ &= \lim_{N\to\infty} \frac{1}{N} \left| \sum_{n=0}^{N-1} x_p^2[n] s_1[n; \hat{\boldsymbol{\theta}}^{(p)}] \right|.\end{aligned} \tag{24}$$

Following [15], it can be shown that

$$\begin{aligned}&\lim_{N\to\infty} \frac{1}{N} \sum_{n=0}^{N-1} x_p^2[n] s_1[n; \hat{\boldsymbol{\theta}}^{(p)}] \\ &\quad = \lim_{N\to\infty} \frac{1}{N} \sum_{n=0}^{N-1} E\{x_p^2[n]\} s_1[n; \hat{\boldsymbol{\theta}}^{(p)}]\end{aligned} \tag{25}$$

and therefore we obtain

$$\begin{aligned}L_\infty(x_p, \hat{\boldsymbol{\theta}}^{(p)}) &= \lim_{N\to\infty} \frac{1}{N} \left| \sum_{n=0}^{N-1} E\{x_p^2[n]\} s_1[n; \hat{\boldsymbol{\theta}}^{(p)}] \right| \\ &= \lim_{N\to\infty} \frac{1}{N} \left| \sum_{n=0}^{N-1} \sum_{m=p}^{2M} \mu_{\tilde{a}_m} \right. \\ &\qquad \left. \cdot s_m[n; \boldsymbol{\theta}] s_1[n; \hat{\boldsymbol{\theta}}^{(p)}] \right|.\end{aligned} \tag{26}$$

The cross-product of two chirps with different parameters is negligible w.r.t. N for a sufficiently large value of N [36]. Therefore

$$L_\infty(x_p, \hat{\boldsymbol{\theta}}^{(p)}) = \left| \sum_{m=p}^{2M} \mu_{\tilde{a}_m} \delta(\hat{\boldsymbol{\theta}}^{(p)} - m\boldsymbol{\theta}) \right|. \tag{27}$$

That is, $L(x_{p+1}, \hat{\boldsymbol{\theta}}^{(p)})/N$ has $2M - p + 1$ peaks at each $m\boldsymbol{\theta}$ for $m = p, \ldots, 2M$ with a magnitude of $\mu_{\tilde{a}_m}$. Since we assume that the components are estimated in order, the last result implies that $\mu_{\tilde{a}_2} > \mu_{\tilde{a}_3} > \cdots > \mu_{\tilde{a}_{2M}}$ and consequently $L(x_p, p\boldsymbol{\theta}) > L(x_p, m\boldsymbol{\theta}),\ \forall m > p$. Therefore we conclude that

$$\arg\max_{\hat{\boldsymbol{\theta}}^{(p)}} \left\{ L_\infty(x_p, \hat{\boldsymbol{\theta}}^{(p)}) \right\} = p\boldsymbol{\theta} \tag{28}$$

and thus the estimator is asymptotically unbiased.

Proposition 1: The asymptotic variance of $\hat{\boldsymbol{\theta}}^{(p)}$ is given by

$$\operatorname{var}(\hat{\theta}_1^{(p)}) = \frac{24}{\pi^2 N^3} \frac{tr\left\{R_a\right\}\sigma_v^2 + 0.5\sigma_v^4}{\mu_{\tilde{a}_p}^2} \tag{29}$$

$$\operatorname{var}(\hat{\theta}_2^{(p)}) = \frac{90}{\pi^2 N^5} \frac{tr\left\{R_a\right\}\sigma_v^2 + 0.5\sigma_v^4}{\mu_{\tilde{a}_p}^2} \tag{30}$$

where R_a is the $M \times M$ cross-correlation matrix of the amplitudes whose elements are given by

$$R_a[k, \ell] = E\{a_k[n] a_\ell[n]\}. \tag{31}$$

Proof: See Appendix A. ■

Proposition 2: For a single harmonic, i.e., $M = 1$, the results (29) and (30) converge to the asymptotic variance presented in [15] for NLSE of a mono-component LFM.

Proof: For $M = 1$, we get that $tr\left\{R_a\right\} = R_a = E\{a_1^2\}$. In addition, $\tilde{a}_1 = a_1^2[n]$ and therefore $\mu_{\tilde{a}_1}^2 = E\{a_1^2\}^2$. Substituting $tr\left\{R_a\right\}$ and $\mu_{\tilde{a}_1}^2$ into (29) and (30) yields the same result as in [15], except for a small difference in the frequency normalization, i.e., a factor of 2π and π for the initial frequency and frequency rate, respectively. ■

So far we obtained the asymptotic bias and variance of the estimator in each step of IHNLSE. In order to evaluate the overall asymptotic bias and variance of IHNLSE, we assume that the estimators are approximately uncorrelated. This is not accurate, but can be assumed since the components are well separated in $L(x, \boldsymbol{\theta})$. Since the mono-component estimator is asymptotically unbiased, it is clear that IHNLSE is also asymptotically unbiased. The asymptotic variance is given by

$$\begin{aligned} \operatorname{var}(\hat{\theta}_1) &= \frac{1}{C_M^2} \sum_{m=2}^{2M} m^2 \cdot \operatorname{var}(\hat{\theta}_1^{(f(m))}) \\ &= \frac{24}{\pi^2 N^3 C_M^2} r_M \end{aligned} \tag{32}$$

$$\begin{aligned} \operatorname{var}(\hat{\theta}_2) &= \frac{1}{C_M^2} \sum_{m=2}^{2M} m^2 \cdot \operatorname{var}(\hat{\theta}_2^{(f(m))}) \\ &= \frac{90}{\pi^2 N^5 C_M^2} r_M \end{aligned} \tag{33}$$

where $r_M = (tr\left\{R_a\right\}\sigma_v^2 + 0.5\sigma_v^4) \sum_{m=2}^{2M} m^2/\mu_{\tilde{a}_m}^2$.

Note that the last result implies that in order to achieve the optimal accuracy, a search resolution of $N^{3/2}$ and $N^{5/2}$ is required for the initial frequency and frequency rate, respectively.

C. Computational Load

We evaluate the computational complexity of IHNLSE by calculating the number of on-line multiplications. Each iteration of the process involves a two-dimensional search. In order to achieve the possible accuracy, the resolutions of the searches for the initial frequency and frequency rate are $1/N^{3/2}$ and $1/N^{5/2}$, respectively. That means that there are an order of $N^{3/2} \cdot N^{5/2}/N = N^3$ search points. Each point requires a calculation of the cost function, $L(x, \boldsymbol{\theta})$, which can be done using $\mathcal{O}(N)$ multiplications. The modulation and filtering of the signal is also performed using $\mathcal{O}(N)$ multiplications. Therefore, the complexity of each iteration is $\mathcal{O}(N^4)$. Since there are $2M - 1$ iterations, the total computational complexity of IHNLSE is $\mathcal{O}(N^4 M)$.

D. Unknown Model Order

As mentioned above, when the number of harmonic components is unknown, a model order selection criterion is required. Methods such as minimum description length (MDL) or Akaike information criterion (AIC) are commonly used and successfully applied to multicomponent and harmonic chirps [36]. Both involve the maximum likelihood cost function [43], which requires estimates of the parameters and amplitudes of each component. Since IHNLSE cannot be used to estimate the amplitudes, these criteria are not useful. We therefore suggest to incorporate a detection process in the IHNLSE to determine the number of components.

Example 1 (Cont.): As an example, to illustrate the idea of this process, Fig. 3 presents the spectrum of $x_m[n]$ for each iteration of the IHNLSE, i.e., $m = 1, \ldots, 2M$, where $x[n]$ is the same signal as in Example 1. Fig. 3(a) shows the spectrum of $x_1[n] = x^2[n]$, with the five harmonic components apparent. After the first iteration, the strongest component is filtered using the process described in the previous subsection, as can be seen in Fig. 3(b). The process is repeated $2M - 1$ times. Finally, when all harmonic components are filtered, the spectrum, showed in Fig. 3(f), has no major peaks and its power is overall lower than the previous iterations.

We can therefore detect the number of harmonic components by examining a peakedness measure of the spectrum of $x_m[n]$. Such measures were presented in [44]. Particularly, we examine the Kurtosis, Hoyer, Shannon entropy (H_S) and Gaussian entropy (H_G) measures. In addition, we examine the energy level of the signal as a measure. Definitions for all measures are presented in Table I for the spectrum of $x_m[n]$, denoted by $X^{(m)}[n]$. The measures for the signal from Example 1 are presented in Fig. 4. The measures are normalized so that they equal 1 at $m = 1$. All measures reach a certain level at $m = 2M$ and change very little afterwards, with the exception of the Gaussian entropy measure which is almost not effected and thus not suitable for our purpose. The number of harmonic components can estimated as

$$\hat{M} = \arg\min_m \left\{Sp(2m) + p_r(2m)\right\} \tag{34}$$

where $Sp(m)$ is a spectrum peakedness measure at the m'th iteration and p_r is a monotonically increasing (w.r.t. m) regularization to prevent over estimation. The iterative harmonic-NLSE

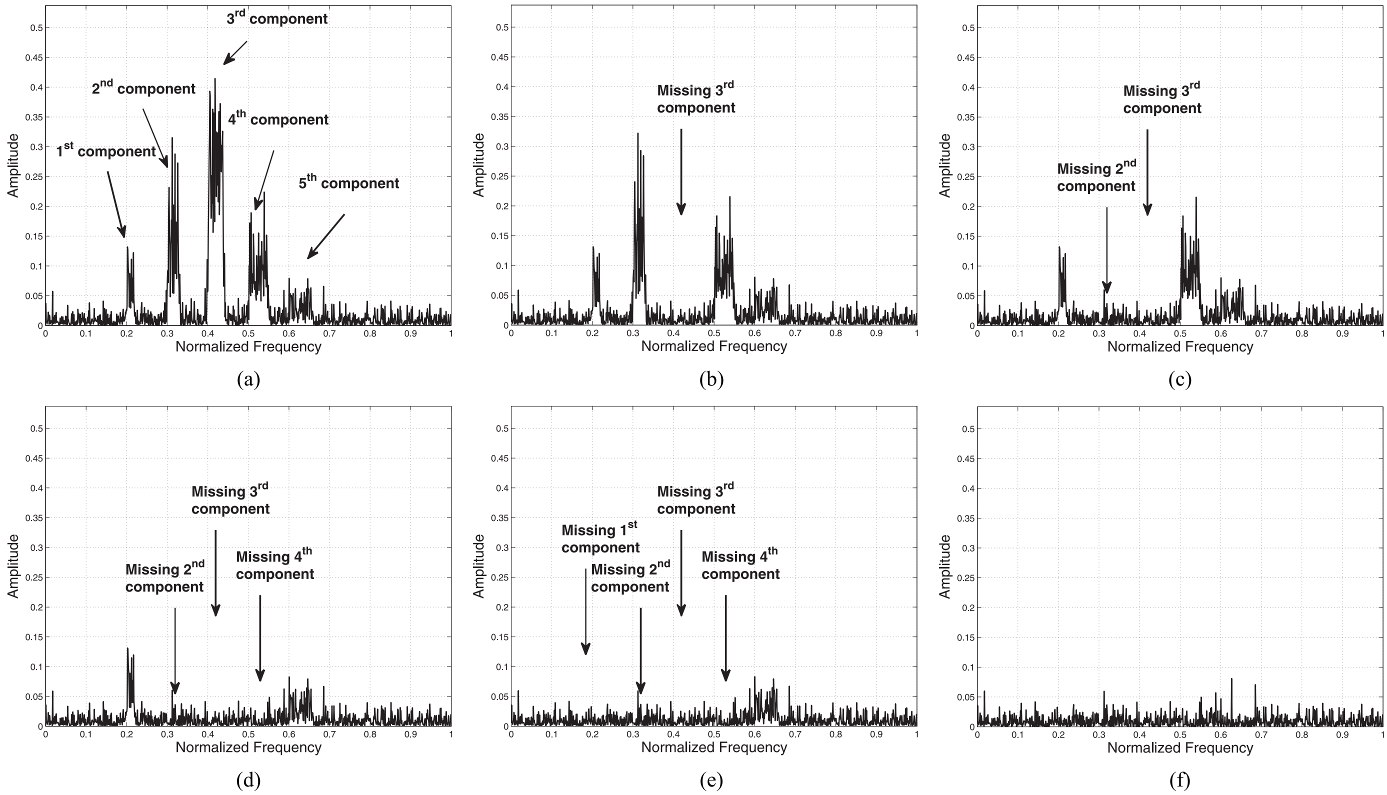

Fig. 3. Spectrum of x_m for (a) $m=1$ (i.e., x^2), (b) $m=2$, (c) $m=3$,(d) $m=4$, (e) $m=5$, and (f) $m=6$ (i.e., $2M$).

with model order selection (IHNLSE-MO) is summarized in Algorithm 2.

Algorithm 2: Iterative Harmonic-NLSE for Unknown Model Order (IHNLSE-MO)

Input:

$x[n]$ – Input signal

D – Maximum possible model order

Output:

$\hat{\boldsymbol{\theta}}$ – Estimated parameters

$\hat{M}$ – Estimated model order

$x_1[n] \leftarrow x^2[n]$

for $m \leftarrow 1, \ldots, D$ **do**

$Sp(m) \leftarrow$ Peakedness measure of $x_m[n]$

$\hat{\boldsymbol{\theta}}^{(m)} \leftarrow \arg\max_{\boldsymbol{\theta}} L(x_m, \boldsymbol{\theta})$

$x_{m+1}[n] \leftarrow ((x_m[n]s^*[n; 2\hat{\boldsymbol{\theta}}^{(m)}]) * h[n])s[n; 2\hat{\boldsymbol{\theta}}^{(m)}]$

end for

$\hat{M} = \arg\min_{m} \{Sp(2m) + p_r(2m)\}$

$\hat{\boldsymbol{\theta}} \leftarrow = \frac{1}{C_{\hat{M}}} \sum_{m=2}^{2\hat{M}} m\hat{\boldsymbol{\theta}}^{(f(m))}$

VI. Low Complexity Estimators

In order to avoid the high-resolution two-dimensional search required for IHNLSE, we present two low-complexity estimators. The first is a modification of HAF estimator [15] for a single component LFM with a random amplitude. The second is a modification of the Harmonic-SEES [36] for constant-amplitude harmonic chirps.

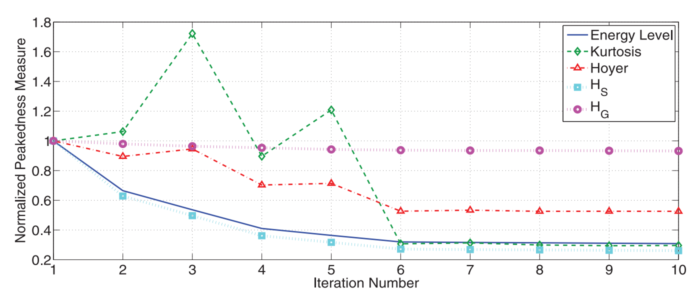

Fig. 4. Peakedness measures and energy level of the spectrum of x_m for Example 1. Measures are normalized so that they equal 1 at $m=1$.

TABLE I
Definition of Peakedness Measures for $X^{(m)}[k]$

Measure	Definition
Energy Level	$\sum_k \lvert X^{(m)}[k]\rvert^2$
Kurtosis	$\frac{\sum_k \lvert X^{(m)}[k]\rvert^4}{(\sum_k \lvert X^{(m)}[k]\rvert^2)^2}$
Hoyer	$\sqrt{N} - \frac{\sum_k \lvert X^{(m)}[k]\rvert}{\sqrt{\sum_k \lvert X^{(m)}[k]\rvert^2}}$
H_S	$\sum_k \lvert X^{(m)}[k]\rvert \log \lvert X^{(m)}[k]\rvert^2$
H_G	$\sum_k \log \lvert X^{(m)}[k]\rvert^2$

A. A Modified HAF Estimator

In order to avoid the high resolution two dimensional search involved in NLSE, a suboptimal estimation method was proposed in [15] based on HAF. We first explain in short the HAF method for a mono-component case. For a single LFM, the discrete ambiguity function is given by

$$\begin{aligned}\rho_k[n] &= x^*[n]x[n+k] \\ &= a[n]a[n+k]e^{j2\pi(\theta_1 k+\frac{1}{2}\theta_2 k^2)}e^{j2\pi(\theta_2 kn)} \\ &\quad + v_\rho[n]\end{aligned} \tag{35}$$

for some constant k, where $v_\rho[n]$ is the transformed noise given by $v_\rho[n] = a[n]^* s^*[n,\boldsymbol{\theta}]v[n+k] + v^*[n]a[n+k]s[n+k,\boldsymbol{\theta}] + v^*[n]v[n+k]$. The signal $\rho_k[n]$ is a sinusoid with a time-varying random amplitude in presence of non-Gaussian noise. The chirp rate, θ_2, can be obtained from ρ_k using the LS approach again. This time, however, the result is a one dimensional search problem. It can be shown that [15]

$$\hat{\theta}_2 = \frac{1}{2k}\arg\max_{\tilde{\theta}_2}\left|\sum_{n=0}^{N-1}\rho_k^2[n]e^{-j2\pi\tilde{\theta}_2 n^2}\right|. \tag{36}$$

Once θ_2 is estimated according to (36), we determine θ_1 as

$$\hat{\theta}_1 = \frac{1}{2k}\arg\max_{\tilde{\theta}_1}\left|\sum_{n=0}^{N-1}x^2[n]e^{-j2\pi\hat{\theta}_2 n^2}e^{-j2\pi\cdot 2\tilde{\theta}_1 n}\right|. \tag{37}$$

Note that (36) and (37) essentially find the maximum of the absolute value of the discrete-time Fourier transform (DTFT) of $\rho_k^2[n]$ and $x^2[n]$, respectively. Additionally, it is worth noting that $\rho_k^2[n]$ is equivalent to the second order ambiguity function of $x^2[n]$. As can be seen, the solution for random-amplitude signal is similar to the constant amplitude except the squaring of the signal, just as in NLSE.

Now, we return to the problem of harmonic signals. We wish to obtain an expression for $\rho_k[n]$:

$$\begin{aligned}\rho_k[n] &= \sum_{m,m'=1}^{M} a_m[n]a_{m'}[n+k]s_m^*[n;\boldsymbol{\theta}]s_{m'}[n+k;\boldsymbol{\theta}] \\ &\quad + v_\rho[n] \\ &= \sum_{m=1}^{M} a_m[n]a_m[n+k]s_m^*[n;\boldsymbol{\theta}]s_m[n+k;\boldsymbol{\theta}] \\ &\quad + \sum_{m\neq m'} a_m[n]a_{m'}[n+k]s_m^*[n;\boldsymbol{\theta}]s_{m'}[n+k;\boldsymbol{\theta}] \\ &\quad + v_\rho[n].\end{aligned} \tag{38}$$

From (35) we know that the first sum results in harmonic sinusoids of order M at frequencies $k\theta_2, 2k\theta_2, \ldots, Mk\theta_2$ with random amplitudes. The second sum in (38) is the cross terms between the harmonic components. Substituting (2) into (38), it can be shown that

$$\begin{aligned}s_m^*[n;\boldsymbol{\theta}]s_{m'}[n+k;\boldsymbol{\theta}] &= e^{j2\pi(m'-m)(\tilde{\theta}_1 n+\frac{1}{2}\theta_2 n^2)} \\ &\quad \cdot e^{-j2\pi m'(\theta_1 k+\frac{1}{2}\theta_2 k^2)}\end{aligned} \tag{39}$$

where $\tilde{\theta}_1 = \theta_1 + m'k\theta_2/(m'-m)$. That is, the cross terms in (38) are also LFM signals. So the problem becomes estimating from $\rho_k[n]$ the fundamental frequency of harmonic sinusoid with random amplitude in presence of the transformed noise and LFM signals. From (38) and (10), it can be shown that $\rho_k^2[n]$ contains random-amplitude harmonic sinusoids of order $2M$ with the fundamental frequency missing. That is, $2M-1$ sinusoids at frequencies $2k\theta_2, 3k\theta_2, \ldots, 2Mk\theta_2$. The LS approach used to obtain (36) and (37), results in maximizing a DTFT. In case of harmonic signals, instead of using DTFT, we apply the idea of the Harmogram [45], a method for estimating the fundamental frequency of an harmonic series of sinusoids. The chirp rate, θ_2, can be estimated using a modified Harmogram criterion

$$\hat{\theta}_2 = \frac{1}{k}\arg\max_{\tilde{\theta}_2}\sum_{m=2}^{2M}\left|\sum_{n=0}^{N-1}\rho_k^2[n]e^{-j2\pi m\tilde{\theta}_2 n^2}\right|. \tag{40}$$

Once $\hat{\theta}_2$ is estimated, we define the set of the following M signals

$$x_m[n] = x[n]e^{j2\pi\frac{m}{2}\hat{\theta}_2 n^2}. \tag{41}$$

This is termed de-chirping since that for $\hat{\theta}_2 = \theta_2$, each $x_m[n]$ is a single sinusoid with random amplitude in the presence of other harmonic components and noise. Finally, θ_1 is estimated using a modified Harmogram approach as well

$$\hat{\theta}_1 = \frac{1}{2}\arg\max_{\tilde{\theta}_1}\sum_{m=1}^{M}\left|\sum_{n=0}^{N-1}x_m^2[n]e^{-j2\pi m\tilde{\theta}_1 n}\right|. \tag{42}$$

Note that for $M = 1$, (40) is clearly the same as (36). Then, by substituting (41) for $m = 1$ into (42), we obtain the exact expression as in (37). That is, for $M = 1$, the solution is exactly the same as the mono-component case.

B. The Harmonic Separate-Estimate Method for Random Amplitudes

The Harmonic-SEES is a low-complexity estimation method for harmonic LFM with constant amplitudes [36]. We now extend the Harmonic-SEES to the random-amplitude model. Similarly to the two previous methods, in order to do so, we define a pre-processing step of squaring the signal, before applying the Harmonic-SEES. As noted before, the squared signal contains $2M$ harmonics but the fundamental component is missing. That is, $2M-1$ components overall. Therefore, the second modification to the Harmonic-SEES is to take into account that the fundamental component, whose parameters are those we wish to estimate, is missing. We provide a short summary of the Harmonic-SEES with the required modifications for random-amplitude model. We term this method HRA-SEES. When the number of harmonic components is known, HRA-SEES method is very similar to the Harmonic-SEES method, and a summary of the method is presented below for clarification. The model order selection for constant-amplitude model involves MDL or AIC criteria. Both are not applicable for this case as explained above. Therefore the model order selection presented in the next subsection differs from [36].

The first step is separating the signal into $2M-1$ harmonic components. This is achieved with a coarse estimation of the parameters. Recall that de-chirping the signal with the appropriate chirp rate yields a sinusoid in presence of other components and noise. The coarse estimation is done by using the fact that the sinusoid will yield a strong peak in the discrete Fourier transform (DFT) of the de-chirped signal. We define a set of L chirp rate candidates, $\{\theta_{2,\ell}\}_{\ell=1}^{L}$. For each candidate, we define $2M-1$ de-chirped signals by

$$x_{\ell,m}[n] = x^2[n]\cdot e^{-j2\pi m\frac{1}{2}\theta_{2,\ell}n^2} \tag{43}$$

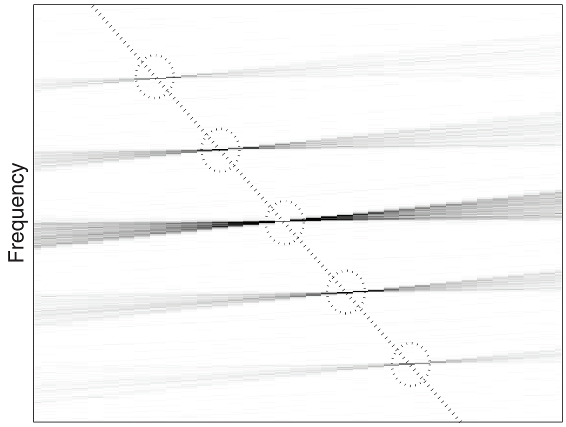

Fig. 5. De-chriping map of $x^2[n]$ for $M = 3$, from Example 1. The 5 peaks are marked in circles aligned on the straight marked line. Note the similarity to Fig. 2, however here it is obtained using DFT.

for $m = 2, \ldots, 2M$. The chirp rate estimate can be obtained as

$$\tilde{\theta}_2 = \arg\max_{\theta_{2,\ell}} \left\{ \max_{0 \le k < N/(2M)} \sum_{m=2}^{2M} |\bar{x}_{\ell,m}[mk]|^2 \right\} \tag{44}$$

where $\bar{x}_{\ell,m}$ is the DFT of $x_{\ell,m}$. Note that k in (44) is the index of the fundamental frequency, and therefore $k < N/(2M)$.

Example 1 (Cont.): We further consider the signal in Example 1, as an illustrative example. By de-chirping with each candidate, and then calculating the magnitude of the DFT of each de-chirped signal, we obtain a de-chirping map. An example of the map is presented in Fig. 5. The map contains $2M - 1 = 5$ peaks marked on the figure. The peaks are aligned on a straight line, also marked on the figure. The chirp rate selection in (44) can be thought of as summing $2M - 1$ equispaced points along a straight line in the map. We note that there is a similarity to Hough-based approaches [46].

Note that this process, as can be seen from the example, is very similar to the NLSE cost function maximization. However, there are two key differences. First, the number of candidate chirp rate required is very small relative to NLSE since this is only a coarse estimate. Second, the use of DFT, rather than the DTFT, reduces the complexity due to its efficient implementation, the fast Fourier transform (FFT). In order to compensate the poor resolution obtained by that process we preform LS estimation given the phase of each component. But first, the components must be separated.

Once the coarse estimation is obtained, the de-chirped harmonic components can be separated from each de-chirped signal, $x_{\ell,m}$. The harmonic components are then reconstructed by a simple chirp multiplication [36].

So far, we obtained a set of $2M - 1$ reconstructed harmonic components, $\{\hat{s}_2[n], \ldots, \hat{s}_{2M}[n]\}$, of the observed signal. The information on the initial frequency and frequency rate is hidden in the phases of the harmonic components. We now can proceed to the second step of estimating the parameters. This is done using a joint phase unwrapping and parameter estimation described in [36] with a simple modification. Since that the fundamental chirp is missing, the linear model of the phases has to be adapted accordingly. That is, we wish to solve the following LS problem

TABLE II
COMPARISON OF THE COMPUTATIONAL LOAD OF THE THREE ESTIMATION METHODS.

Method	Complexity
IHNLSE	$\mathcal{O}\left(N^4 M\right)$
HAF	$\mathcal{O}(N^{5/2} M)$
HRA-SEES	$\mathcal{O}\left(N^2 \log NM\right)$

$$[\{\hat{\tilde{\varphi}}_m\}_{m=2}^{2M}, \hat{\boldsymbol{\theta}}^T]^T = \arg\min_{\{\tilde{\varphi}_m\},\boldsymbol{\theta}} \sum_{m=2}^{2M} \|\tilde{\boldsymbol{\phi}}_m - \tilde{\varphi}_m \mathbf{1}_N - 2\pi m \mathbf{H}\boldsymbol{\theta}\|^2 \tag{45}$$

where $\tilde{\boldsymbol{\phi}}_m$ is the unwrapped phase of the m'th component, $\mathbf{1}_N$ is the $N \times 1$ vector with all elements equal to one and $\mathbf{H} = [\mathbf{h}_1, \mathbf{h}_2]$ with $\mathbf{h}_1 = [0, 1, \ldots, N-1]^T$, and $\mathbf{h}_2 = [0^2/2, 1^2/2, \ldots, (N-1)^2/2]^T$. The estimate of $\boldsymbol{\theta}$ is given by [36]

$$\hat{\boldsymbol{\theta}} = (\mathbf{H}^T \mathbf{P}_1^{\perp} \mathbf{H})^{-1} \mathbf{H}^T \mathbf{P}_1^{\perp} \boldsymbol{\Psi} \tag{46}$$

where $\mathbf{P}_1^{\perp} = \mathbf{I}_N - \mathbf{1}_N (\mathbf{1}_N^T \mathbf{1}_N)^{-1} \mathbf{1}_N^T$ is an orthogonal projection matrix, $\boldsymbol{\Psi} = \frac{1}{2\pi C_M} \sum_{m=2}^{2M} m \tilde{\boldsymbol{\phi}}_m$ and C_M is defined in (20).

C. Computational Load

We first evaluate the computational complexity of HAF based method. HAF reduces the problem to two one-dimensional problems, but does not change the search resolution required to achieve optimal performance. The construction of the cost function in (40) requires $\mathcal{O}(NM)$ multiplications per frequency. The number of frequency rates required is in the order of $N^{5/2}/N$. The total number of multiplications required for the frequency rate estimation is therefore $\mathcal{O}(N^{5/2}M)$. Next, M DTFTs are required, one for each de-chirped signal. The number of frequencies in this step is in the order of $N^{3/2}$. The complexity of the initial frequencies estimation is therefore $\mathcal{O}(N^{5/2}M)$. To conclude, HAF method involves $\mathcal{O}(N^{5/2}M)$ multiplications, a significant improvement over the computational load of IHNLSE.

The computational complexity of HRA-SEES method is exactly the same as the Harmonic-SEES method, i.e., $\mathcal{O}\left(N^2 \log NM\right)$ on-line multiplications [36], which is better than both IHNLSE and HAF methods. The computational loads of all three estimators are summarized in Table II.

D. Unknown Model Order

So far, in both low-complexity estimation methods, the number of harmonic components was assumed to be known. Therefore, similarly to IHNLSE, a model order selection rule is required. IHNLSE works iteratively. That is, in each step one component is estimated and removed. However, both low-complexity methods suggested using all the components at once. Thus, the methods must be applied for every possible M. Using the same approach as in IHNLSE, for a given M, once the parameters are estimated, M harmonic components are filtered from the original signal, $x[n]$, using the same de-modulation scheme. Note that in this case the filtering is performed on $x[n]$ rather than $x^2[n]$ as in IHNLSE. Again, peakedness measures of the spectrum of the filtered signal can be calculated to obtain a model order selection criterion. The model order selection framework is summarized in Algorithm 3. The estimation step can be achieved either with HAF-based estimation or with the suggested HRA-SEES method.

Algorithm 3: Model Order Selection Framework

Input:
$x[n]$ – Input signal
D – Maximum possible model order

Output:
$\hat{\boldsymbol{\theta}}$ – Estimated parameters
$\hat{M}$ – Estimated model order

for $m = 1$ to D **do**
  Estimate parameters of $x[n]$, $\hat{\boldsymbol{\theta}}^{(m)}$, assuming m harmonics.
  $x^{(m)}[n] \leftarrow x[n]$
  for $k = 1$ to m **do**
    $x^{(m)}[n] \leftarrow ((x^{(m)}[n]s^*[n;k\hat{\boldsymbol{\theta}}^{(m)}]) * h[n])s[n;k\hat{\boldsymbol{\theta}}^{(m)}]$
  end for
  $Sp(m) \leftarrow$ Peakedness measure of $x_m[n]$
end for
$\hat{M} \leftarrow \underset{m=1,\ldots,D}{\arg\min}\ \{Sp(m) + p_r(m)\}$
$\hat{\boldsymbol{\theta}} \leftarrow \hat{\boldsymbol{\theta}}^{(\hat{M})}$

VII. Piece-Wise Continuity

In practice, the signals are often long and processed in segments. The input signal is windowed, and the signal in (1) is used to model a single segment, or observation window. We assume that each segment can be approximated by a series of harmonic LFM signals but the entire signal can be any other model, for example higher-order polynomial phase signals (PPS).

So far, we have treated the problem of estimating the frequency of the fundamental component of a single segment, without any prior knowledge. However, the fact that the fundamental frequency should be smooth, can be exploited by imposing a piece-wise continuity constraint, which means that the initial frequency of each segment should be very close to the final frequency of the previous segment. Moreover, it can be expected that the frequency rate should not change significantly between two consecutive segments.

Denote by $\hat{\boldsymbol{\theta}}_k = [\hat{\theta}_{1,k}, \hat{\theta}_{2,k}]^T$ the estimated parameters of the signal at the k'th segment for $k = 1,\ldots,K$ where K is the number of segments. Denote by $\Omega_{p,k}(m)$ the set of all possible values for the parameters of the mth harmonic component, $\hat{\theta}_{p,k}^{(m)},\ p = 1, 2,$

$$\Omega_{1,k}(m) = \left\{\hat{\theta}_{1,k} : |\hat{\theta}_{1,k}^{(m)} - m\hat{\theta}_{f,k-1}| < \delta_1\right\} \tag{47}$$

$$\Omega_{2,k}(m) = \left\{\hat{\theta}_{2,k} : |\hat{\theta}_{2,k}^{(m)} - m\hat{\theta}_{2,k-1}| < \delta_2\right\} \tag{48}$$

for $k = 2,\ldots,K$ and $m = 2,\ldots,2M$, where $\hat{\theta}_{f,k-1} = \hat{\theta}_{1,k-1} + N\hat{\theta}_{2,k-1}$ is the estimated final frequency of the ($k-1$)'th segment and δ_1 and δ_2 are the maximum allowed differences between segments.

Our objective is to impose the piece-wise continuity constraint in each estimation method. We start with IHNLSE, which involves the following two dimensional maximization problem in Algorithm 1

$$\hat{\boldsymbol{\theta}}_k^{(m)} = \arg\max_{\boldsymbol{\theta}} \frac{1}{N} L(x_m, \boldsymbol{\theta}). \tag{49}$$

Substituting (47) and (48) into (49) yields a new optimization problem given by

$$\hat{\boldsymbol{\theta}}_k^{(m)} = \arg\max_{\boldsymbol{\theta}\in\Omega_k^{(2M)}} \frac{1}{N} L(x_m, \boldsymbol{\theta}) \tag{50}$$

where $\Omega_k^{(2M)}$ is the space of all possible parameters for all harmonic component, i.e.,

$$\Omega_k^{(2M)} = \left\{\hat{\boldsymbol{\theta}}_k : \begin{array}{c} \theta_{1,k} \in \Omega_{1,k}(m), \\ \theta_{2,k} \in \Omega_{2,k}(m) \\ m = 2,\ldots,2M \end{array}\right\}. \tag{51}$$

Similarly, in HAF-based method the piece-wise continuity constraint can be imposed in the optimization problems in (40) and (42),

$$\hat{\theta}_{2,k} = \frac{1}{k} \arg\max_{\tilde{\theta}_2\in\Omega_{2,k}} \sum_{m=2}^{2M} \left| \sum_{n=0}^{N-1} \rho_k^2[n] e^{-j2\pi m\tilde{\theta}_2 n^2} \right| \tag{52}$$

$$\hat{\theta}_{1,k} = \frac{1}{2} \arg\max_{\tilde{\theta}_1\in\Omega_{1,k}} \sum_{m=1}^{M} \left| \sum_{n=0}^{N-1} x_m^2[n] e^{-j2\pi m\tilde{\theta}_1 n} \right|. \tag{53}$$

Both IHNLSE and HAF methods require searching through the parameters space in order to maximize the cost function. Therefore, the constraints simply reduce the search range.

Finally, in HRA-SEES, the constraint can be imposed in the LS problem in the final step, i.e., (45),

$$[\{\hat{\tilde{\varphi}}_m\}, \hat{\boldsymbol{\theta}_k}^T]^T = \underset{\{\tilde{\varphi}_m\},\boldsymbol{\theta}\in\Omega_k}{\arg\min} \sum_{m=2}^{2M} \|\tilde{\boldsymbol{\phi}}_m - \tilde{\varphi}_m \mathbf{1}_N - 2\pi m\mathbf{H}\boldsymbol{\theta}\|^2 \tag{54}$$

where

$$\Omega_k = \left\{\hat{\boldsymbol{\theta}}_k : \begin{array}{c} \theta_{1,k} \in \Omega_{1,k}(1), \\ \theta_{2,k} \in \Omega_{2,k}(1) \end{array}\right\}. \tag{55}$$

Note that (54) is no longer a simple LS problem but a quadratic programming problem, which can be solved, for example, using the reflective Newton method [47]. This is an iterative method, based on Newton's method, that generates a descending (w.r.t. to the cost function) and feasible sequence that convergence to the optimal solution in quadratic rate. Feasibility is ensured by reflecting infeasible points around the boundaries of the feasible region.

VIII. Numerical Results

A. Simulations

We now present examples to compare the performances of IHNLSE, HAF and HRA-SEES methods. In all of the example we consider a signal with $M = 3$ harmonic components and the parameters of the fundamental chirp are given by $\theta_1 = 0.15$ and $\theta_2 = 10^{-5}$. The number of samples is $N = 1024$. The

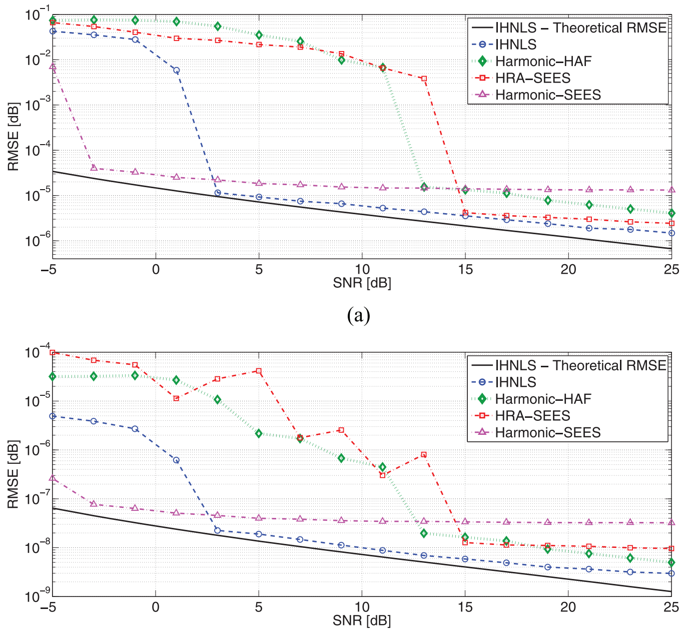

(a)

(b)

Fig. 6. RMSE of each estimator vs. SNR for normally distributed amplitudes. (a) θ_1, Normalized initial frequency. (b) θ_2, Normalized frequency rate.

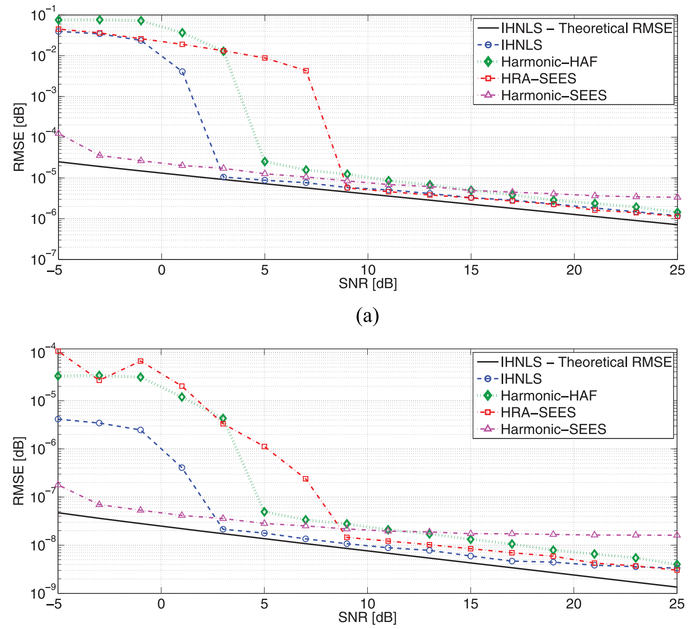

(a)

(b)

Fig. 7. RMSE of each estimator vs. SNR for AR(2) amplitudes. (a) θ_1, Normalized initial frequency. (b) θ_2, Normalized frequency rate.

phases of all component, φ_m, are generated from a uniform distribution, i.e., $\varphi_m \sim U(0, 2\pi)$. We consider two different models for the random amplitude. The first model is of normally distributed amplitudes, in which $\alpha_m[n] \sim \mathcal{N}(1, 0.25)$. In the second model each amplitude is an AR(2) process with parameters $\{1, 0.97, -0.35\}$. The noise power σ_v^2 is adjusted to give the desired SNR defined as $\text{SNR} = 10\log_{10}\left(E\{x^2\}/\sigma_v^2\right) = 10\log_{10}\left(tr\left\{R_a\right\}/\sigma_v^2\right)$ [dB], where $E\{\cdot\}$ denotes the expectation operator. In all simulations we use a lag of $\tau = N/2$ samples in HAF-based estimation method [15].

We start by evaluating the root mean squared error (RMSE) of the estimators when the number of harmonic components is known. The RMSE is defined as $\text{RMSE}(\theta_k) = \sqrt{\frac{1}{Nexp}\sum_{i=1}^{N_{exp}}(\hat{\theta}_{k,i} - \theta_k)^2}$, $k = 1, 2$ where $\hat{\theta}_{1,i}$ and $\hat{\theta}_{2,i}$ are the estimate of θ_1 and θ_2 at the ith trial, respectively and $N_{exp} = 500$ is the number of Monte-Carlo independent trials. Simulation results for the normally distributed amplitudes and AR(2) amplitudes are presented in Figs. 6 and 7, respectively. The results include the RMSE for each estimator and the theoretical RMSE of IHNLSE is plotted. In addition, we include the RMSE of the Harmonic-SEES estimator, that assumes constant amplitudes. As can be expected, IHNLSE yields the best results and almost achieves the theoretical RMSE for SNR above 3 dB. The difference between the theoretical and actual errors can be accounted for by the approximations and assumptions used in deriving the theoretical error. HAF-based estimator and the HRA-SEES method perform similarly. HAF has a slightly better threshold SNR while the HRA-SEES has a slightly better RMSE. Both low-complexity methods fail to achieve the performance of IHNLSE for the normally distributed amplitudes, but still achieve very low errors w.r.t. to the values of the parameters and can be used to initiate a two dimensional search of IHNLSE. The Harmonic-SEES method performed worse in high SNR, due to the inaccurate assumption of constant amplitudes. However, its threshold SNR is lower. This is probably because that in low SNR the squared noise in the random-amplitude methods becomes very strong.

Next we evaluate the model order selection criteria, by calculating the probability of selecting the correct number of harmonic components for various values of SNR. The probability, p_d, is defined as $p_d = \frac{1}{Nexp}\sum_{i=1}^{N_{exp}} \mathbb{1}_{\hat{M}=M}$. The regularization, $p_r(m)$, used is defined by $p_r(m) = m/c_p$ where c_p is a normalization constant to ensure $\sum p_r(m) = 1$. Simulation results for the normally distributed amplitudes and AR(2) amplitudes are presented in Figs. 8 and 9, respectively. For both HAF-based estimation and the HRA-SEES method, there is very little difference between the performance for the different peakedness measures. For IHNLSE, the Shannon entropy and the energy level criteria perform better than the others.

Finally, we wish to examine the sensitivity of each estimator to errors in the model order selection. For that purpose we evaluate the RMSE of each estimator for various values of $\hat{M}$. Simulation results for the normally distributed amplitudes and AR(2) amplitudes are presented in Figs. 10 and 11, respectively. Both IHNLSE and HRA-SEES are very sensitive to errors in the model order selection, while the HAF-based estimator allows errors in the number of harmonic components.

B. Real Data

We now demonstrate the HRA-SEES method with the model order selection for estimating the parameters of two real-data examples of echolocation calls of a bat and a whale [28], [29]. The same examples were used in [36], where the amplitudes assumed to be constant at each observation window. The signals are divided into segments of $N = 1000$ samples. At each segment the parameters and the number of harmonic components are estimated using the HRA-SEES method with the Shannon entropy measure. The piece-wise continuity constraints were

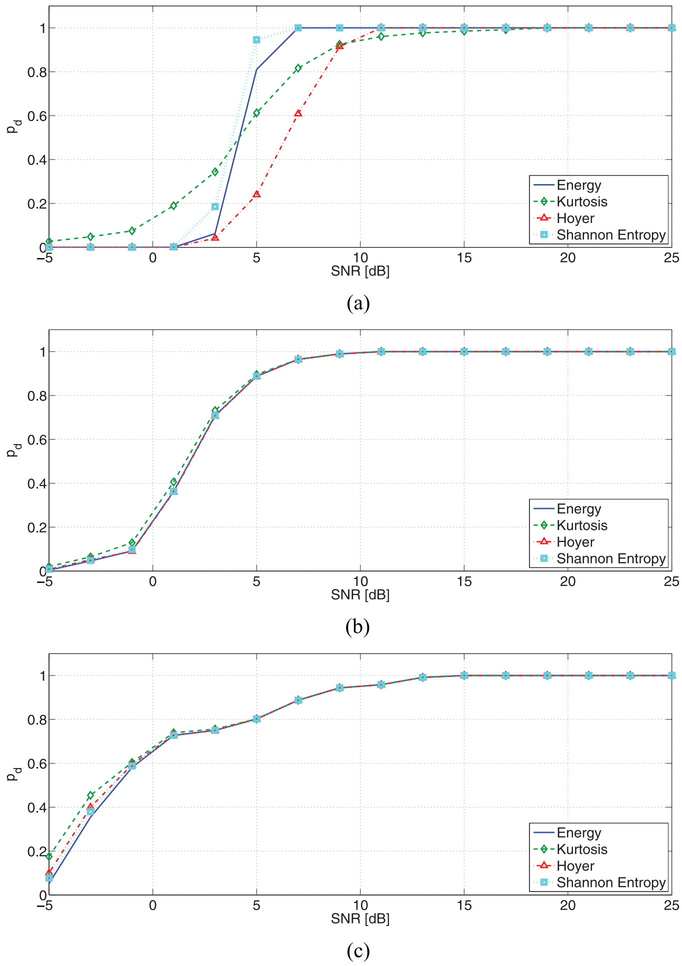

Fig. 8. p_d of each estimator vs. SNR for normally distributed amplitudes. (a) IHNLSE. (b) HAF. (c) HRA-SEES.

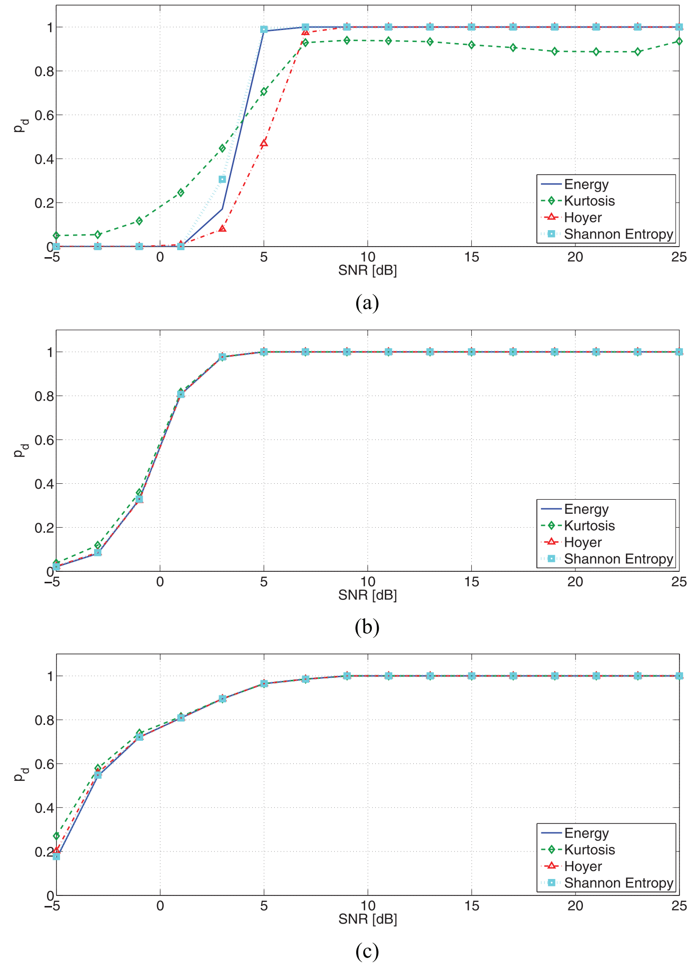

Fig. 9. p_d of each estimator vs. SNR for AR(2) amplitudes. (a) IHNLSE. (b) HAF. (c) HRA-SEES.

$\delta_1 = 1 \cdot 10^{-4}$ and $\delta_2 = 1 \cdot 10^{-6}$. The quadratic programming problem was solved using the reflective Newton method [47].

The first example is an echolocation call produced by an *E. nilssonii* bat [28]. The signal is about 40 ms long and is sampled at $F_s = 250$ kHz. A spectrogram of the signal is presented in Fig. 12. The call has four harmonic components with the last one being very weak. The estimated frequencies are plotted in dashes line on top of the spectrogram and the selected model order is plotted above. The markers on the spectrogram corresponds to a peak detection at each time frame. The peak detection shows that the fundamental chirp is not the most dominant. However, the HRA-SEES method successfully estimated the correct fundamental frequency at each observation window.

The second example is an echolocation call produced by a *G. melas* whale [29]. The signal is about 600 ms long and is sampled to $F_s = 44.1$ kHz. The results are presented in Fig. 13 in the same format as the previous example. The fundamental frequency line is detected in all segments.

We next examine the effect of the constrained optimization and the necessity of the model order selection. Fig. 14 presents the frequency estimates of the *G. melas* whale for constrained and unconstrained optimization techniques with a fixed number of components versus model order selection. The number of components in the fixed part was set to $M = 3$. Clearly, the constrained optimization with model order selection yields the best

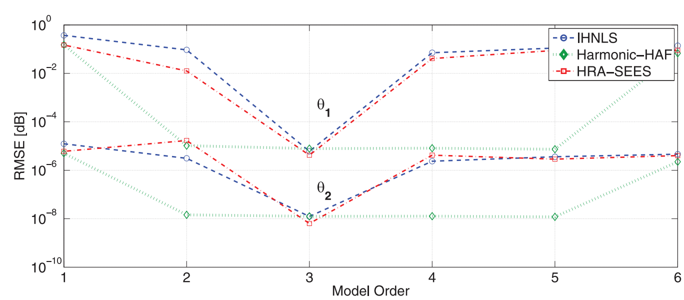

Fig. 10. Sensitivity of the estimators to errors in the model order for normally distributed amplitudes.

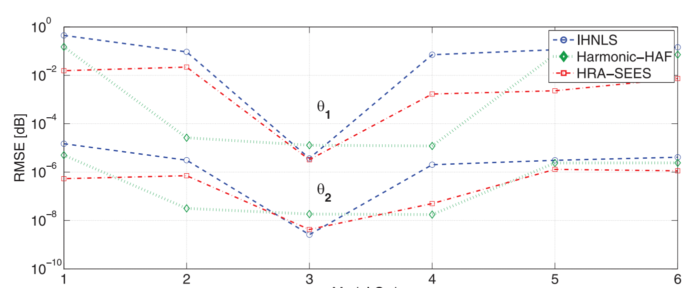

Fig. 11. Sensitivity of the estimators to errors in the model order for AR(2) amplitudes.

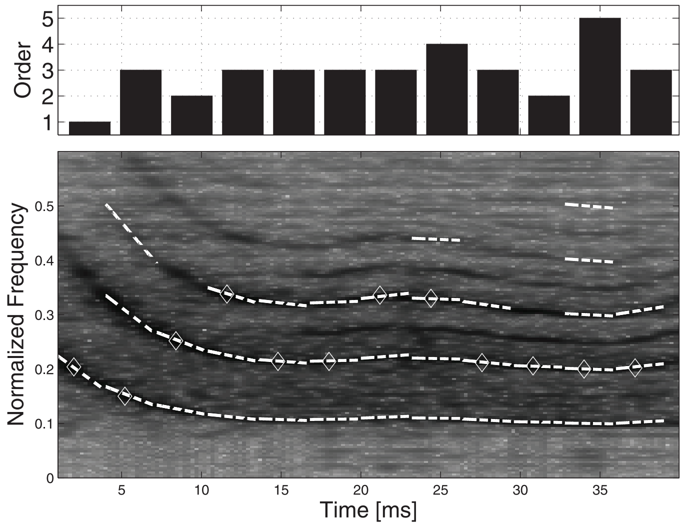

Fig. 12. Model order selection and parameter estimation of an echolocation call produced by a *E. Nilssonii* bat. The diamonds mark peak detection in the spectrogram.

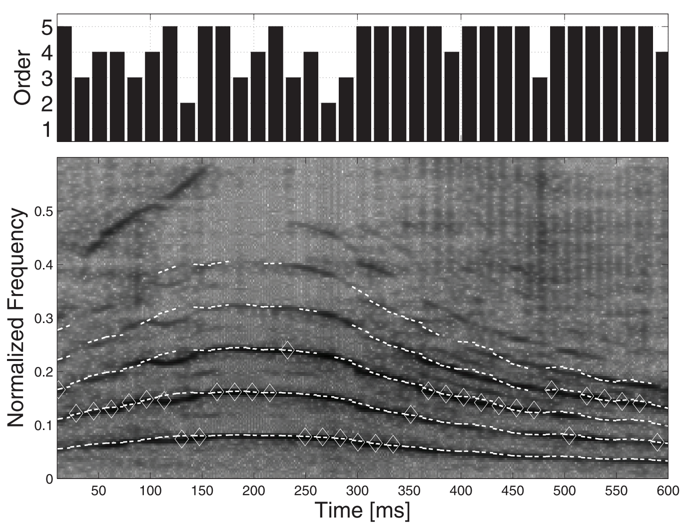

Fig. 13. Model order selection and parameter estimation of an echolocation call produced by a *G. melas* whale. The diamonds mark peak detection in the spectrogram.

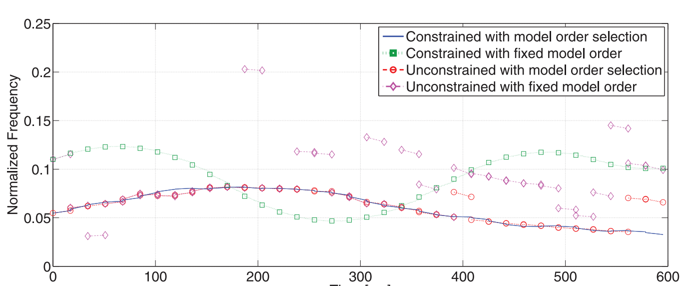

Fig. 14. Comparison of frequency estimates for constrained and unconstrained optimization techniques with fixed or variable model order.

results. The unconstrained optimization with model order estimates the fundamental frequency correctly in all but two segments. Using a fixed number of harmonic components results in poor estimation results. The constrained optimization estimate fails in the first segment. Due to the constraints, the failure of the first segment affects the estimation in the rest of the signal. The unconstrained optimization with a fixed number of components detects the correct fundamental frequency in about half of the segments.

IX. Conclusion

A. Summary

We considered the problem of estimating the parameters of the fundamental frequency of harmonic LFM with random amplitudes when the number of harmonic components is unknown. We suggested three estimation methods. The first is an iterative method based on NLSE, which requires a two-dimensional high resolution search. The second is a modification of HAF-based estimation for mono-component LFM, and the third is a modification of the Harmonic-SEES for harmonic LFM with random amplitudes. We showed through simulations that IHNLSE achieves its asymptotic variance at medium to high SNR and that the two low-complexity methods perform well in high SNR. We also showed that peakedness measures of the spectrum of the signal can be successfully used in order to estimate the number of components in all three methods.

B. Future Research

The work presented herein can be further extended in a number of interesting directions. In this work we assumed that the signal can be modeled as a sum of harmonic LFM components in each observation window. Thus, we allow longer segments, compared to existing methods that assume constant frequency model. We can further increase the segment length by assuming a model of harmonic PPS. The difficulty in doing so is with the first step of the coarse estimation. Currently, this is done by searching for the optimal de-chirping, which for Pth order PPS would require $P-1$ dimensional search. A possible approach to obtain the coarse estimation is to extend the quasi-maximum-likelihood [8], originally proposed for mono-component PPS, to multi-component signals.

Another possibility is to employ frequency tracking. The piece-wise continuity constraints ensure that the frequency estimates are smooth. However, the constraints do not exploit the structure of the signal. For example, we can assume that the signal is a high order PPS and predict, using Kalman filtering, the parameters for the next step. The prediction can replace the first step of de-chirping selection. Moreover, at the end of the process the state variable will provide the estimated parameters of the PPS.

Appendix
Derivation of the NLS Asymptotic Variance

In this section we derive the asymptotic variance of NLSE for harmonic linear chirps. Recall the signal of interest at a single iteration of NLSE $x_{p+1}^2[n] = \tilde{a}_p[n]s_p[n;\boldsymbol{\theta}] + \tilde{v}_p[n]$ for some $p \in \{2,\ldots,2M\}$ and

$$\tilde{v}_p[n] = \sum_{m=2}^{p-1} \bar{a}_m[n] + \sum_{m=p+1}^{2M} \tilde{a}_m[n]s_m[n;\boldsymbol{\theta}] + 2\sum_{m=1}^{M} a_m[n]s_m[n;\boldsymbol{\theta}]v[n] + v^2[n] \quad (56)$$

is an additive non Gaussian noise. We now derive the second order statistics of the noise. The second moment of that noise is given by

$$\begin{aligned}
&E\left\{\tilde{v}_p[n]\tilde{v}_p^*[n']\right\}\\
&=E\left\{\sum_{m=2}^{p-1}\bar{a}_m[n]\tilde{v}_p^*[n']\right\}+E\left\{v^2[n]\left(v^2[n']\right)^*\right\}\\
&\quad+E\left\{\sum_{m=p+1}^{2M}\tilde{a}_m[n]s_m[n;\boldsymbol{\theta}]\sum_{k=p+1}^{2M}\tilde{a}_k^*[n']s_k^*[n';\boldsymbol{\theta}]\right\}\\
&\quad+E\left\{4\sum_{m=1}^{M}a_m[n]s_m[n;\boldsymbol{\theta}]v[n]\right.\\
&\quad\left.\cdot\sum_{k=1}^{M}a_k^*[n']s_k^*[n';\boldsymbol{\theta}]v^*[n']\right\}\\
&\quad+E\left\{2\sum_{m=p+1}^{2M}\Re\{\tilde{a}_m[n]s_m[n;\boldsymbol{\theta}]\right.\\
&\quad\left.\cdot\sum_{k=1}^{M}a_k^*[n']s_k^*[n';\boldsymbol{\theta}]v^*[n']\}\right\}\\
&\quad+E\left\{\sum_{m=p+1}^{2M}\Re\{\tilde{a}_m[n]s_m[n;\boldsymbol{\theta}]\left(v^2[n']\right)^*\}\right\}\\
&\quad+E\left\{2\sum_{m=1}^{M}\Re\{a_m[n]s_m[n;\boldsymbol{\theta}]v[n]\left(v^2[n']\right)^*\}\right\}. \qquad (57)
\end{aligned}$$

Since $v[n]$ is a zero-mean circularly-symmetric complex normal variable, $E\left\{v^*[n']v^2[n]\right\}=0$ and $E\left\{v^2[n]\right\}=0$. In addition, the noise is assumed to be uncorrelated with the amplitudes. Hence,

$$E\left\{\tilde{a}_m[n]s_m[n;\boldsymbol{\theta}]a_k^*[n']s_k^*[n';\boldsymbol{\theta}]v^*[n']\right\}=0 \qquad (58)$$
$$E\left\{\tilde{a}_m^*[n']s_m^*[n';\boldsymbol{\theta}]a_k[n]s_k[n;\boldsymbol{\theta}]v[n]\right\}=0 \qquad (59)$$
$$E\left\{\tilde{a}_m[n]s_m[n;\boldsymbol{\theta}]\left(v^2[n']\right)^*\right\}=0 \qquad (60)$$
$$E\left\{\tilde{a}_m^*[n']s_m^*[n';\boldsymbol{\theta}]v^2[n]\right\}=0 \qquad (61)$$
$$E\left\{a_m[n]s_m[n;\boldsymbol{\theta}]v[n]\left(v^2[n']\right)^*\right\}=0 \qquad (62)$$
$$E\left\{a_m^*[n']s_m^*[n';\boldsymbol{\theta}]v^*[n']v^2[n]\right\}=0 \qquad (63)$$

for any $m,k\in\{1,\ldots,M\}$. Recall that $E\{\bar{a}_m[n]\}=0$. Therefore

$$E\left\{\sum_{m=2}^{p-1}\bar{a}_m[n]\tilde{v}_p^*[n']\right\}=\sum_{m=2}^{p-1}E\left\{\bar{a}_m[n]\bar{a}_m[n']\right\}\delta(n-n'). \qquad (64)$$

Assuming that the amplitudes are uncorrelated, we get

$$\begin{aligned}
&E\left\{\sum_{m=1}^{M}a_m[n]s_m[n;\boldsymbol{\theta}]v[n]\sum_{k=1}^{M}a_k^*[n']s_k^*[n';\boldsymbol{\theta}]v^*[n']\right\}\\
&=E\left\{\sum_{m=1}^{M}a_m[n]a_m^*[n']\right\}\sigma_v^2\delta(n-n')\\
&=(tr\left\{R_a\right\}\sigma_v^2)\delta(n-n') \qquad (65)
\end{aligned}$$

where R_a is the cross-correlation matrix of the amplitudes whose elements are given by $R_a[k,\ell]=E\{a_k[n]a_\ell^*[n]\}$. Therefore we obtain

$$\begin{aligned}
E\left\{\tilde{v}_p[n]\tilde{v}_p^*[n']\right\}&=(4tr\left\{R_a\right\}\sigma_v^2+2\sigma_v^4)\delta(n-n')\\
&\quad+\left(\sum_{m=2}^{p-1}E\left\{\bar{a}_m[n]\bar{a}_m^*[n']\right\}\right)\delta(n-n')\\
&\quad+\sum_{m=p+1}^{2M}\sum_{k=p+1}^{2M}E\left\{\tilde{a}_m[n]\tilde{a}_k^*[n']\right\}\\
&\quad\cdot s_m[n;\boldsymbol{\theta}]s_k^*[n';\boldsymbol{\theta}]. \qquad (66)
\end{aligned}$$

Similarly it can be shown that

$$\begin{aligned}
E\left\{\tilde{v}_p[n]\tilde{v}_p[n']\right\}=&\sum_{m=p+1}^{2M}\sum_{k=p+1}^{2M}E\left\{\tilde{a}_m[n]\tilde{a}_k[n']\right\}\\
&\cdot s_m[n;\boldsymbol{\theta}]s_k[n';\boldsymbol{\theta}]\\
&+\sum_{m=2}^{p-1}E\left\{\bar{a}_m[n]\bar{a}_m[n']\right\}\delta(n-n'). \qquad (67)
\end{aligned}$$

As noted in [15], the optimization problem in (6), used to estimate the parameters of $x_p^2[n]$ is equivalent to

$$\{\hat{\boldsymbol{\theta}}^{(p)},\hat{A}_p\}=\arg\min_{\boldsymbol{\theta},A_p}\left|\sum_{n=0}^{N-1}x_p^2[n]-A_pe^{-j2m\pi(\theta_1n+\frac{1}{2}\theta_2n^2)}\right|^2. \qquad (68)$$

where A_p is constant such that $\hat{A}_p\to\mu_{\tilde{a}_p}$, and $\mu_{\tilde{a}_p}=E\{\tilde{a}_p\}$. Following the same steps as in [15, Appendix B], it can be shown that

$$\mathrm{var}\left(\psi^{(p)}\right)=\frac{1}{\mu_{\tilde{a}_p}^2}\Lambda_N^{-1}R_\epsilon\Lambda_N^{-1} \qquad (69)$$

where $\psi^{(p)}=[\tilde{\varphi}_p,(\hat{\boldsymbol{\theta}}^{(p)})^T]^T$,

$$\Lambda_N=\pi^2\begin{bmatrix}N^{1/2}\cdot 1 & N^{1/2}\cdot 2/2 & N^{1/2}\cdot 1/3\\ N^{3/2}\cdot 2/2 & N^{3/2}\cdot 4/3 & N^{3/2}\cdot 2/4\\ N^{5/2}\cdot 1/3 & N^{5/2}\cdot 2/4 & N^{5/2}\cdot 1/5\end{bmatrix} \qquad (70)$$

and

$$\begin{aligned}
R_\epsilon(k,\ell)=\lim_{N\to\infty}&\frac{g(k)g(\ell)}{8N}\sum_{n,n'=0}^{N-1}\left(\frac{n}{N}\right)^k\left(\frac{n'}{N}\right)^\ell\\
&\cdot\Re\{E\left\{\tilde{v}_p[n]\tilde{v}_p^*[n']\right\}-E\left\{\tilde{v}_p[n]\tilde{v}_p[n']\right\}\} \qquad (71)
\end{aligned}$$

for $k,\ell=0$, 1, 2, where $g(k)$ is the frequency normalization for each parameter, i.e., $g(0)=1$ for the constant phase, $g(1)=2\pi$ for the initial frequency and $g(2)=\pi$ for the frequency rate. Note that (70) and (71) are different from [15] due to different frequency normalization, but otherwise similar. Substituting (66) and (67) into (71) yields

$$\begin{aligned} R_\epsilon(k,\ell) = &\lim_{N\to\infty} \frac{g(k)g(\ell)}{8N} \sum_{n,n'=0}^{N-1} \left(\frac{n}{N}\right)^k \left(\frac{n'}{N}\right)^\ell \\ &\cdot \left[(4tr\left\{R_a\right\}\sigma_v^2 + 2\sigma_v^4)\delta(n-n') \right. \\ &+ 2\sum_{m=p+1}^{2M}\sum_{k=p+1}^{2M} E\left\{\tilde{a}_m[n]\tilde{a}_k[n']\right\} \\ &\left.\cdot \Im\{s_m[n;\boldsymbol{\theta}]\}\Im\{s_k[n';\boldsymbol{\theta}]\}\right]. \end{aligned} \tag{72}$$

In order get a large sample approximation of the result, we assume that $E\left\{\tilde{a}_m[n]\tilde{a}_k[n']\right\}$ is time independent. That is, we assume the $E\left\{\tilde{a}_m[n]\tilde{a}_k[n']\right\} = R_{m,k}$ for any m, k. This assumption holds, for example, when the amplitudes are independent and normally distributed. We now wish to examine the elements in the sum in (72)

$$\begin{aligned} &\lim_{N\to\infty}\frac{1}{N}\sum_{n,n'=0}^{N-1}\left(\frac{n}{N}\right)^k\left(\frac{n'}{N}\right)^\ell E\left\{\tilde{a}_m[n]\tilde{a}_k[n']\right\} \\ &\quad\cdot \Im\{s_m[n;\boldsymbol{\theta}]\}\Im\{s_k[n';\boldsymbol{\theta}]\} \\ &= R_{m,k}\lim_{N\to\infty}\frac{1}{N}\sum_{n,n'=0}^{N-1}\left(\frac{n}{N}\right)^k\left(\frac{n'}{N}\right)^\ell \\ &\quad\cdot \Im\{s_m[n;\boldsymbol{\theta}]\}\Im\{s_k[n';\boldsymbol{\theta}]\} \\ &< R_{m,k}\lim_{N\to\infty}\frac{1}{N}\sum_{n,n'=0}^{N-1}\Im\{s_m[n;\boldsymbol{\theta}]\}\Im\{s_k[n';\boldsymbol{\theta}]\} \\ &= R_{m,k}\underbrace{\lim_{N\to\infty}\frac{1}{N}\sum_{n=0}^{N-1}\Im\{s_m[n;\boldsymbol{\theta}]\}}_{\to 0} \\ &\quad\cdot\sum_{n=0}^{N-1}\Im\{s_k[n';\boldsymbol{\theta}]\} \\ &\underset{N\to\infty}{\to} 0. \end{aligned} \tag{73}$$

Therefore, for large number of samples we get

$$\begin{aligned} R_\epsilon(k,\ell) &\approx \lim_{N\to\infty}\frac{g(k)g(\ell)}{8N}\sum_{n,n'=0}^{N-1}\left(\frac{n}{N}\right)^k\left(\frac{n'}{N}\right)^\ell \\ &\quad\cdot(4tr\left\{R_a\right\}\sigma_v^2+2\sigma_v^4)\delta(n-n') \\ &= (4tr\left\{R_a\right\}\sigma_v^2+2\sigma_v^4)\lim_{N\to\infty}\frac{1}{8N}\sum_{n=0}^{N-1}\left(\frac{n}{N}\right)^{k+\ell} \\ &= (tr\left\{R_a\right\}\sigma_v^2+0.5\sigma_v^4)\frac{g(k)g(\ell)}{2(k+\ell+1)}. \end{aligned} \tag{74}$$

Finally, substituting (74) into (69) yields (29) and (30). This concludes the derivation of the asymptotic variance of NLSE.

Acknowledgment

The authors would like to thank the associate editor and the anonymous reviewers for their insightful and constructive comments which helped to improve and clarify the paper.

References

[1] S. Peleg and B. Porat, "Estimation and classification of polynomial-phase signals," *IEEE Trans. Inf. Theory*, vol. 37, no. 2, pp. 422–430, Mar. 1991.

[2] S. Peleg and B. Friedlander, "Multicomponent signal analysis using the polynomial-phase transform," *IEEE Trans. Aerosp. Electron. Syst.*, vol. 32, no. 1, pp. 378–387, Jan. 1996.

[3] S. Barbarossa, A. Scaglione, and G. Giannakis, "Product high-order ambiguity function for multicomponent polynomial-phase signal modeling," *IEEE Trans. Signal Process.*, vol. 46, no. 3, pp. 691–708, Mar. 1998.

[4] P. Wang, I. Djurovic, and J. Yang, "Generalized high-order phase function for parameter estimation of polynomial phase signal," *IEEE Trans. Signal Process.*, vol. 56, no. 7, pp. 3023–3028, Jul. 2008.

[5] P. Wang, H. Li, I. Djurovic, and B. Himed, "Instantaneous frequency rate estimation for high-order polynomial-phase signals," *IEEE Signal Process. Lett.*, vol. 16, no. 9, pp. 782–785, Sep. 2009.

[6] D. S. Pham and A. M. Zoubir, "Analysis of multicomponent polynomial phase signals," *IEEE Trans. Signal Process.*, vol. 55, no. 1, pp. 56–65, Jan. 2007.

[7] P. O'Shea, "Improving polynomial phase parameter estimation by using nonuniformly spaced signal sample methods," *IEEE Trans. Signal Process.*, vol. 60, no. 7, pp. 3405–3414, Jul. 2012.

[8] I. Djurović and L. Stanković, "Quasi-maximum-likelihood estimator of polynomial phase signals," *IET Signal Process.*, vol. 8, no. 4, pp. 347–359, Jun. 2014.

[9] B. Barkat and B. Boashash, "Instantaneous frequency estimation of polynomial FM signals using the peak of the PWVD: Statistical performance in the presence of additive Gaussian noise," *IEEE Trans. Signal Process.*, vol. 47, no. 9, pp. 2480–2490, Sep. 1999.

[10] L. Qi, R. Tao, S. Zhou, and Y. Wang, "Detection and parameter estimation of multicomponent LFM signal based on the fractional Fourier transform," *Sci. in China Series F, Inf. Sci.*, vol. 47, no. 2, pp. 184–198, Mar. 2004.

[11] G. Zhou and G. Giannakis, "Harmonics in multiplicative and additive noise: Performance analysis of cyclic estimators," *IEEE Trans. Signal Process.*, vol. 43, no. 6, pp. 1445–1460, Jun. 1995.

[12] O. Besson and P. Stoica, "Sinusoidal signals with random amplitude: Least-squares estimators and their statistical analysis," *IEEE Trans. Signal Process.*, vol. 43, no. 11, pp. 2733–2744, Nov. 1995.

[13] S. Shamsunder, G. Giannakis, and B. Friedlander, "Estimating random amplitude polynomial phase signals: A cyclostationary approach," *IEEE Trans. Signal Process.*, vol. 43, no. 2, pp. 492–505, Feb. 1995.

[14] A. Swami, "Cramer-rao bounds for deterministic signals in additive and multiplicative noise," *Signal Process.*, vol. 53, no. 2–3, pp. 231–244, Sep. 1996.

[15] O. Besson, M. Ghogho, and A. Swami, "Parameter estimation for random amplitude chirp signals," *IEEE Trans. Signal Process.*, vol. 47, no. 12, pp. 3208–3219, Dec. 1999.

[16] M. Morelande and A. Zoubir, "On the performance of cyclic moments-based parameter estimators of amplitude modulated polynomial phase signals," *IEEE Trans. Signal Process.*, vol. 50, no. 3, pp. 590–606, Mar. 2002.

[17] P. Tsiakoulis and A. Potamianos, "Statistical analysis of amplitude modulation in speech signals using an AM-FM model," in *Proc. IEEE Int. Conf. Acoust., Speech, Signal Process. (ICASSP)*, Apr. 2009, pp. 3981–3984.

[18] M. Pineda-Sanchez, M. Riera-Guasp, J. Roger-Folch, J. Antonino-Daviu, J. Perez-Cruz, and R. Puche-Panadero, "Diagnosis of induction motor faults in time-varying conditions using the polynomial-phase transform of the current," *IEEE Trans. Ind. Electron.*, vol. 58, no. 4, pp. 1428–1439, Apr. 2011.

[19] O. Besson and P. Stoica, "Nonlinear least-squares approach to frequency estimation and detection for sinusoidal signals with arbitrary envelope," *Digit. Signal Process.*, vol. 9, no. 1, pp. 45–56, Jan. 1999.

[20] M. Ghogho, A. Swami, and A. Nandi, "Non-linear least squares estimation for harmonics in multiplicative and additive noise," in *Proc. 9th IEEE SSAP Workshop*, Sep. 1998, pp. 407–410.

[21] O. Besson and P. Stoica, "Two subspace-based methods for frequency estimation of sinusoidal signals with random amplitude," *Proc. Inst. Elect. Eng., Radar, Sonar, Navig.*, vol. 144, no. 4, pp. 169–176, Aug. 1997.

[22] G. Zhou and G. Giannakis, "On estimating random amplitude-modulated harmonics using higher order spectra," *IEEE J. Ocean. Eng.*, vol. 19, no. 4, pp. 529–539, Oct. 1994.

[23] A. Swami, “Multiplicative noise models: Parameter estimation using cumulants,” *Signal Processing*, vol. 36, no. 3, pp. 355–373, Apr. 1994.
[24] M. Ghogho, A. Swami, and T. Durrani, “Frequency estimation in the presence of Doppler spread: Performance analysis,” *IEEE Trans. Signal Process.*, vol. 49, no. 4, pp. 777–789, Apr. 2001.
[25] G. Zhou, G. Giannakis, and A. Swami, “On polynomial phase signals with time-varying amplitudes,” *IEEE Trans. Signal Process.*, vol. 44, no. 4, pp. 848–861, Apr. 1996.
[26] B. Barkat and B. Boashash, “IF estimation of linear FM signals corrupted by multiplicative and additive noise: A time-frequency approach,” in *Proc. IEEE Int. Conf. Acoust., Speech, Signal Process. (ICASSP)*, Istanbul, Turkey, Jun. 2000, vol. 2, pp. 661–664.
[27] B. Barkat, “Instantaneous frequency estimation of nonlinear frequency-modulated signals in the presence of multiplicative and additive noise,” *IEEE Trans. Signal Process.*, vol. 49, no. 10, pp. 2214–2222, Oct. 2001.
[28] G. Pfalzer, Avisoft Bioacoustics, European Bat Calls [Online]. Available: http://www.batcalls.com
[29] *Interdisciplinary Center for Bioacoustics and Environmental Research*, [Online]. Available: http://www.unipv.it/cibra/
[30] S. Raimund, Avisoft Bioacoustics [Online]. Available: http://www.avisoft.com
[31] T. H. Chung and J. Cheung, “Maximum likelihood estimation of direction of arrival and frequency sweeping rate with linear chirp signals,” *IEEE Signal Process. Lett.*, vol. 2, no. 8, pp. 163–165, Aug. 1995.
[32] R. Aouada, A. Belouchrani, and K. Abed-Meraim, “Multipath parameter estimation of linear chirp signals using sensor arrays,” in *Proc. IEEE Sensor Array Multichannel Signal Process. Workshop (SAM)*, Jul. 2004, pp. 313–317.
[33] M. Bennett, S. McLauglin, T. Anderson, and N. McDicken, “Filtering of chirped ultrasound echo signals with the fractional Fourier transform,” in *Proc. IEEE Ultrason. Symp.*, Aug. 2004, vol. 3, pp. 2036–2040.
[34] M. Vespe, G. Jones, and C. Baker, “Lessons for radar: Waveform diversity in echolocating mammals,” *IEEE Signal Process. Mag.*, vol. 26, no. 1, pp. 65–75, Jan. 2009.
[35] Y. Kopsinis, E. Aboutanios, D. A. Waters, and S. McLaughlin, “Time-frequency and advanced frequency estimation techniques for the investigation of bat echolocation calls,” *J. Acoust. Soc. Amer.*, vol. 127, no. 2, pp. 1124–1134, Feb. 2010.
[36] Y. Doweck, A. Amar, and I. Cohen, “Joint model order selection and parameter estimation of chirps with harmonic components,” *IEEE Trans. Signal Process.*, vol. 63, no. 7, pp. 1765–1778, Apr. 2015.
[37] Y. Doweck, A. Amar, and I. Cohen, “Parameter estimation of harmonic linear chirps,” in *Proc. 2015 Eur. Signal Process. Conf. (EUSIPCO)*, Nice, France, Sep. 2015, pp. 1491–1495.
[38] A. Amar, A. Leshem, and A. J. van der Veen, “A low complexity blind estimator of narrowband polynomial phase signals,” *IEEE Trans. Signal Process.*, vol. 58, no. 9, pp. 4674–4683, Sep. 2010.
[39] A. Amar, A. Leshem, and A. J. van der Veen, “A computationally efficient blind estimator of polynomial phase signals observed by a sensor array,” in *Proc. IEEE Sensor Array Multichannel Signal Process. Workshop (SAM)*, Oct. 2010, pp. 253–256.
[40] J. Wood and D. Barry, “Radon transformation of time-frequency distributions for analysis of multicomponent signals,” *IEEE Trans. Signal Process.*, vol. 42, no. 11, pp. 3166–3177, Nov. 1994.
[41] M. Wang, A. K. Chan, and C. K. Chui, “Linear frequency-modulated signal detection using Radon-ambiguity transform,” *IEEE Trans. Signal Process.*, vol. 46, no. 3, pp. 571–586, Mar. 1998.
[42] M. Polad and B. Friedlander, “Separation of co-channel FM/PM signals using the discrete polynomial-phase transform,” in *Sixth IEEE Digit. Signal Process. Workshop*, Oct. 1994, pp. 3–6.
[43] H. Van Trees*, Detection, Estimation, and Modulation Theory – Part IV, Optimum Array Processing*. New York, NY, USA: Wiley, 2004.
[44] N. Hurley and R. Scott, “Comparing measures of sparsity,” *IEEE Trans. Inf. Theory*, vol. 55, no. 10, pp. 4723–4741, Oct. 2009.
[45] M. Hinich, “Detecting a hidden periodic signal when its period is unknown,” *IEEE Trans. Acoust., Speech, Signal Process.*, vol. 30, no. 5, pp. 747–750, Oct. 1982.
[46] S. Barbarossa, “Analysis of multicomponent LFM signals by a combined Wigner-Hough transform,” *IEEE Trans. Signal Process.*, vol. 43, no. 6, pp. 1511–1515, Jun. 1995.
[47] T. F. Coleman and Y. Li, “A reflective Newton method for minimizing a quadratic function subject to bounds on some of the variables,” *SIAM J. Optim.*, vol. 6, no. 4, pp. 1040–1058, 1996.

Yaron Doweck (S’14) received the B.Sc. degree (*cum laude*) in electrical engineering in 2012 from the Technion – Israel Institute of Technology.

In 2010 he joined the Signal Processing Department at Rafael, Haifa. He is currently pursuing the M.Sc. degree in Electrical Engineering at the Technion. His research interests are statistical signal processing and array processing.

Alon Amar (S’04–M’09) received the B.Sc. degree (*cum laude*) in electrical engineering from the Technion – Israel Institute of Technology, in 1997, and the M.Sc. and Ph.D. degrees in electrical engineering from Tel Aviv University, Tel Aviv, Israel, in 2003, and 2009, respectively.

Between 2009 and 2010 he was a Postdoctoral Research Associate with the Circuits and Systems group, Faculty of Electrical Engineering, Mathematics and Computer Science, Delft University of Technology, Delft, The Netherlands. In 2011 he joined Rafael as a Research Scientist at the Signal Processing Department. His main research interests include array signal processing, wireless communication, and sensor networks.

Israel Cohen (M’01-SM’03-F’15) is a Professor of electrical engineering at the Technion—Israel Institute of Technology, Haifa, Israel. He received the B.Sc. (*summa cum laude*), M.Sc. and Ph.D. degrees in electrical engineering from the Technion—Israel Institute of Technology, in 1990, 1993 and 1998, respectively.

From 1990 to 1998, he was a Research Scientist with RAFAEL Research Laboratories, Haifa, Israel Ministry of Defense. From 1998 to 2001, he was a Postdoctoral Research Associate with the Computer Science Department, Yale University, New Haven, CT, USA. In 2001 he joined the Electrical Engineering Department of the Technion. He is a coeditor of the Multichannel Speech Processing Section of the *Springer Handbook of Speech Processing* (Springer, 2008), a coauthor of *Noise Reduction in Speech Processing* (Springer, 2009), a Coeditor of *Speech Processing in Modern Communication: Challenges and Perspectives* (Springer, 2010), and a General Cochair of the 2010 International Workshop on Acoustic Echo and Noise Control (IWAENC). He served as Guest Editor of the *European Association for Signal Processing Journal on Advances in Signal Processing* Special Issue on Advances in Multimicrophone Speech Processing and the*Elsevier Speech Communication Journal* a Special Issue on Speech Enhancement. His research interests are statistical signal processing, analysis and modeling of acoustic signals, speech enhancement, noise estimation, microphone arrays, source localization, blind source separation, system identification and adaptive filtering.

Dr. Cohen was a recipient of the Alexander Goldberg Prize for Excellence in Research, and the Muriel and David Jacknow Award for Excellence in Teaching. He serves as a member of the IEEE Audio and Acoustic Signal Processing Technical Committee and the IEEE Speech and Language Processing Technical Committee. He served as Associate Editor of the IEEE TRANSACTIONS ON AUDIO, SPEECH, and LANGUAGE PROCESSING and IEEE SIGNAL PROCESSING LETTERS.